Synthesis, Characterisation, Crystal Structures, Reactivity, and Electrochemistry of Ruthenium – Nitrido, Ruthenium – Cobalt – Imido and Ruthenapyrrolidone Carbonyl Clusters Containing Alkyne Ligands

Emmie Ngai-Man Ho,[a] Zhenyang Lin,[b] and Wing-Tak Wong*[a]

Abstract: Thermolysis of $[Ru_3(CO)_9(\mu_3\text{-}NOMe)(\mu_3\text{-}\eta^2\text{-}PhC_2Ph)]$ (**1**) with two equivalents of $[Cp^*Co(CO)_2]$ in THF afforded four new clusters, brown $[Ru_5(CO)_8(\mu\text{-}CO)_3(\eta^5\text{-}C_5Me_5)(\mu_5\text{-}N)(\mu_4\text{-}\eta^2\text{-}PhC_2Ph)]$ (**2**), green $[Ru_3Co_2(CO)_7(\mu_3\text{-}CO)(\eta^5\text{-}C_5Me_5)_2(\mu_3\text{-}NH)\{\mu_4\text{-}\eta^8\text{-}C_6H_4C(H)C(Ph)\}]$ (**3**), orange $[Ru_3(CO)_7(\mu\text{-}\eta^6\text{-}C_5Me_4CH_2)\{\mu\text{-}\eta^3\text{-}PhC_2(Ph)C(O)N(OMe)\}]$ (**4**) and pale yellow $[Ru_2(CO)_6\{\mu\text{-}\eta^3\text{-}PhC_2(Ph)C(O)N(OMe)\}]$ (**5**). Cluster **2** is a pentaruthenium μ_5-nitrido complex, in which the five metal atoms are arranged in a novel "spiked" square-planar metal skeleton with a quadruply bridging alkyne ligand. The μ_5-nitrido N atom exhibits an unusually low frequency chemical shift in its ^{15}N NMR spectrum. Cluster **3** contains a triangular Ru_2Co – imido moiety linked to a ruthenium – cobaltocene through the $\mu_4\text{-}\eta^8\text{-}C_6H_4C(H)C(Ph)$ ligand. Clusters **4** and **5** are both metallapyrrolidone complexes, in which interaction of diphenylacetylene with CO and the NOMe nitrene moiety were observed. In **4**, one methyl group of the Cp* ring is activated and interacts with a ruthenium atom. The "distorted" Ru_3Co butterfly nitrido complex $[Ru_3Co(CO)_5(\eta^5\text{-}C_5Me_5)(\mu_4\text{-}N)(\mu_3\text{-}\eta^2\text{-}PhC_2Ph)(\mu\text{-}I)_2I]$ (**6**) was isolated from the reaction of **1** with $[Cp^*Co(CO)I_2]$ heated under reflux in THF, in which a Ru–Ru wing edge is missing. Two bridging and one terminal iodides were found to be placed along the two Ru–Ru wing edges and at a hinge Ru atom, respectively. The redox properties of the selected compounds in this study were investigated by using cyclic voltammetry and controlled potential coulometry. ^{15}N magnetic resonance spectroscopy studies were also performed on these clusters.

Keywords: cluster compounds · cobalt · N ligands · NMR spectroscopy · ruthenium

Introduction

Mixed-metal clusters have been increasingly used in catalysis over the last three decades, and there is evidence that cooperative effects may lead to improved properties when compared with homometallic systems.[1–3] The presence of different metals in the same complex may have synergistic effects in catalytic activity.[4, 5] The application of the isolobal analogy[6] and the development of metal-exchange reactions[7] by Stone and Vahrenkamp, respectively, are two successful approaches to the rational synthesis of heterometallic clusters. Another established strategy is the use of an assembling ligand to assist cluster build-up, by the coordination of additional metal-ligand fragments. In this way low nuclearity complexes that contain alkyne ligands can be employed as precursors for the construction of higher nuclearity alkyne clusters.[8–10] Besides, ligand-bridged cluster complexes with alkynes have revealed a tendency for the alkyne ligands to bond to the bridging ligands.[10–12]

We have examined the reactions of the methoxynitrido carbonyl cluster $[Ru_3(CO)_9(\mu_3\text{-}CO)(\mu_3\text{-}NOMe)]$ with alkyne ligands; this resulted in the isolation of a series of nitrene/nitrido clusters $[Ru_3(CO)_9(\mu_3\text{-}NOMe)(\mu_3\text{-}\eta^2\text{-}PhC_2R')]$, $[Ru_4(CO)_9(\mu\text{-}CO)_2(\mu_4\text{-}NR)(\mu_4\text{-}\eta^2\text{-}PhC_2R')]$ (R = H, OMe or C(O)OMe; R′ = H or Ph) and $[Ru_6(CO)_{13}(\mu\text{-}H)(\mu_5\text{-}N)(\mu_3\text{-}\eta^2\text{-}PhC_2Ph)_2]$ in moderate yields.[9, 10] It has also shown that the reactivity of $[Ru_3(CO)_9(\mu_3\text{-}NOMe)(\mu_3\text{-}\eta^2\text{-}PhC_2R')]$ differs markedly from those of its precursors $[Ru_3(CO)_9(\mu_3\text{-}CO)(\mu_3\text{-}NOMe)]$ and $[Ru_3(\mu\text{-}H)_2(CO)_9(\mu_3\text{-}NOMe)]$, both of which have been extensively studied.[13–15] We also found that the treatment of triruthenium methoxynitrido carbonyl clusters with mononuclear cobalt complexes resulted in N–O bond scission and led to butterfly Ru_3Co nitrido clusters in high yields.[16, 17] Reaction of $[Ru_3Co(\mu\text{-}H)(\eta^5\text{-}C_5Me_5)(CO)_9(\mu_4\text{-}N)]$ with alkynes to give a square-planar μ_4-NH cluster is

[a] Dr. W.-T. Wong, E. N.-M. Ho
Department of Chemistry, The University of Hong Kong
Pokfulam Road, Hong Kong (P. R. China)
Fax: (+852) 2547-2933 or (+852) 2857-1586
E-mail: wtwong@hkucc.hku.hk

[b] Dr. Z. Lin
Department of Chemistry
The Hong Kong University of Science and Technology
Clear Water Bay, Kowloon, Hong Kong (P. R. China)

0947-6539/01/0701-0258 $ 17.50+.50/0

observed.[16] These findings prompted us to examine cluster building and ligand rearrangement by the reaction of an alkyne-containing cluster $[Ru_3(CO)_9(\mu_3\text{-NOMe})(\mu_3\text{-}\eta^2\text{-}PhC_2Ph)]$ (**1**) with $[Cp^*Co(CO)_2]$ and $[Cp^*Co(CO)I_2]$.

Results and Discussion

Synthesis, structure and spectroscopy—reaction of $[Ru_3(CO)_9(\mu_3\text{-NOMe})(\mu_3\text{-}\eta^2\text{-}PhC_2Ph)]$ (1) with $[Cp^*Co(CO)_2]$: A solution mixture of $[Ru_3(CO)_9(\mu_3\text{-NOMe})(\mu_3\text{-}\eta^2\text{-}PhC_2Ph)]$ (**1**) and two equivalents of $[Cp^*Co(CO)_2]$ heated under reflux in THF darkens to a colour near black over a 12 hour period. Chromatographic separation of the product mixture gave, in order of elution, trace amounts of red $[Ru_4(CO)_{12}(\mu_4\text{-}\eta^2\text{-}PhC_2Ph)]$,[18] yellow $[Ru_4(CO)_9(\mu\text{-CO})_2(\mu_4\text{-NOMe})(\mu_4\text{-}\eta^2\text{-}PhC_2Ph)]$[10] and purple $[Ru_2Co(CO)_6(\mu_3\text{-CO})(\eta^5\text{-}C_5Me_5)(\mu_3\text{-NH})]$,[16] brown $[Ru_5(CO)_8(\mu\text{-CO})_3(\eta^5\text{-}C_5Me_5)(\mu_5\text{-N})(\mu_4\text{-}\eta^2\text{-}PhC_2Ph)]$ (**2**) (15%), yellow $[Ru_4(CO)_9(\mu\text{-CO})_2(\mu_4\text{-NH})(\mu_4\text{-}\eta^2\text{-}PhC_2Ph)]$[19] (10%), brown $[Ru_3Co(CO)_6(\mu\text{-CO})_2(\eta^5\text{-}C_5Me_5)(\mu_4\text{-NH})(\mu_4\text{-}\eta^2\text{-}PhC_2Ph)]$[16] (12%), green $[Ru_3Co_2(CO)_7(\mu_3\text{-CO})(\eta^5\text{-}C_5Me_5)_2(\mu_3\text{-NH})\{\mu_4\text{-}\eta^8\text{-}C_6H_4C(H)C(Ph)\}]$ (**3**) (3%), orange $[Ru_3(CO)_7(\mu\text{-}\eta^6\text{-}C_5Me_4CH_2)\{\mu\text{-}\eta^3\text{-}PhC_2(Ph)C(O)N(OMe)\}]$ (**4**) (26%) and pale yellow $[Ru_2(CO)_6\{\mu\text{-}\eta^3\text{-}PhC_2(Ph)C(O)N(OMe)\}]$ (**5**) (8%) (see Scheme 1). The structures of clusters **2**–**4** were unambiguously established by single-crystal X-ray diffraction analyses and supported by ^1H and ^{15}N NMR, IR and electronic absorption spectroscopy as well as FAB mass spectrometry (Table 1). While the crystallisation of cluster **5** met with little success, it was characterised by various spectroscopic methods. These compounds are essentially stable in air in the solid state and have varying degrees of stability in *n*-hexane.

Complex **2** readily crystallised from a brown fraction. The positive FAB mass spectrum of **2** displayed a parent envelope at m/z 1140 with an isotopic distribution consistent with the presence of five ruthenium atoms. The IR spectrum of the compound shows the vibration absorptions for both terminal and bridging carbonyl ligands. The presence of a C_5Me_5 group was apparent from ^1H NMR spectroscopy (singlet at $\delta = 1.29$), while integration of the resonances in the aromatic region suggested the presence of a diphenylacetylene ligand (two Ph groups). The ^{15}N NMR spectrum exhibited a single resonance at $\delta = 381.5$ (s), which is consistent with the presence of a nitrido ligand. The UV-visible absorption maxima and corresponding molar absorption coefficients of **2** in CH_2Cl_2 are listed in Table 1. Two shoulder electronic absorption bands at 320 nm and 400 nm are revealed for cluster **2**. The structure of **2** was determined by a single-crystal X-ray diffraction analysis, and a molecule is shown in Figure 1. Selected bond lengths and angles are given in Table 2.

Compound **2** consists of five metal atoms arranged in a manner that can be described as a square planar with a "spiked" atom Ru(5) attached to Ru(4). A μ_5-nitrido N atom and a quadruply bridging alkyne lie on opposite sides of the Ru_4 square. This Ru_5 metal skeleton is seldom observed, and the interstitial nitride atom occupies an unusual type of cavity, in which it is connected to all five metal atoms. The structures of most of the nitrido clusters (T-shaped, butterfly, square pyramidal and octahedral) are related by an octahedral (or part thereof) geometry about the nitrogen.[20] The notable exceptions are the hexanuclear nitrido clusters of the cobalt triad (trigonal prismatic),[21] the $PtRh_{10}$ mixed-metal nitrido

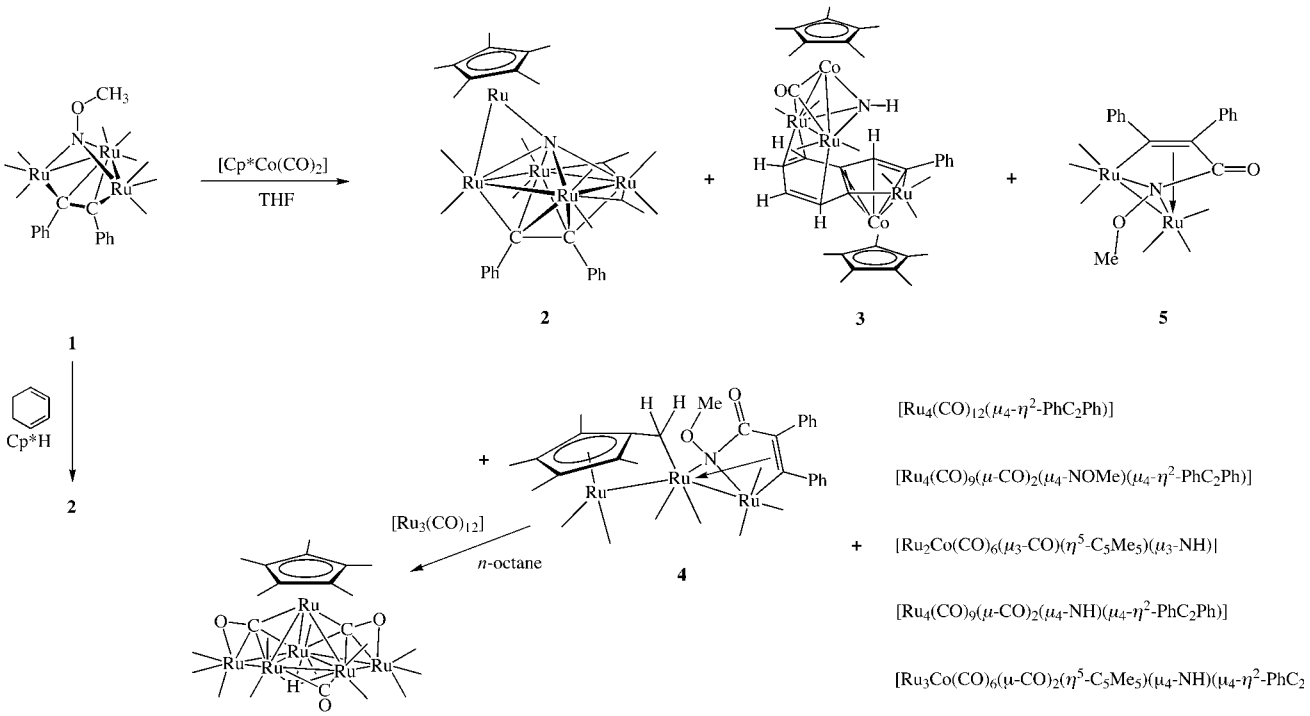

Scheme 1. Treatment of cluster **1** with two equivalents of $[Cp^*Co(CO)_2]$ led to the formation of the new clusters **2**, **3**, **4** and **5** in 15%, 3%, 26% and 8% yields, respectively. Cluster **2** was also directly synthesized from the reaction of **1** with pentamethylcyclopentadiene and 1,3-cyclohexadiene in low yield (4%). Thermolysis of cluster **4** with $[Ru_3(CO)_{12}]$ in *n*-octane lead to the isolation of the known $[Ru_6(\mu_3\text{-H})(CO)_{12}(\mu\text{-CO})(\mu_4\text{-}\eta^2\text{-CO})_2(\eta^5\text{-}C_5Me_5)]$ cluster.

  0947-6539/01/0701-0259 $ 17.50+.50/0

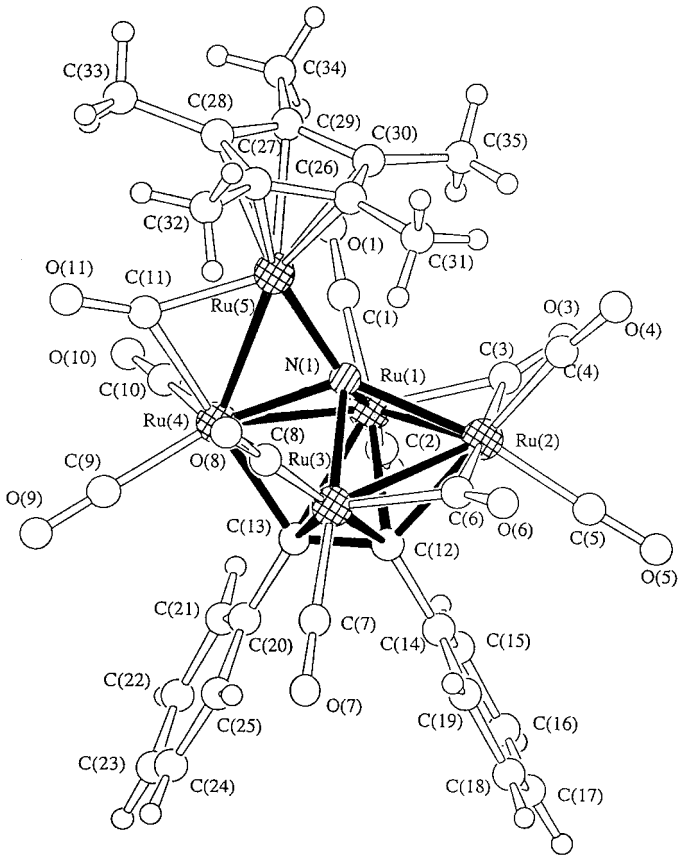

Figure 1. The molecular structure of $[Ru_5(CO)_8(\mu\text{-}CO)_3(\eta^5\text{-}C_5Me_5)(\mu_5\text{-}N)(\mu_4\text{-}\eta^2\text{-}PhC_2Ph)]$ (**2**) with the atom numbering scheme.

cluster (trigonal bipyramidal surrounding N)[22] and the hexaruthenium–nitrido cluster (wing-tip-bridged butterfly surrounding N).[10] The molecule of **2** contains an approximate plane of symmetry that passes through the Ru(2), Ru(4), Ru(5), N(1), C(12) and C(13). Ignoring the rotational conformation of the phenyl rings, the overall structure conforms to the C_s point group. The ruthenium–ruthenium bond lengths span a small range, 2.6363(8)–2.7701(7) Å, which are appreciably shorter relative to those of the Ru–Ru single bond in $[Ru_3(CO)_{12}]$ (2.8555 Å).[23] The shortest bonds contain the edge-bridging carbonyl ligands, and the shortest of these is Ru(4)–Ru(5) [2.6363(8) Å]. This shortening could be due to the existence of a localised multiple bond or the influence of the bridging carbonyl ligand.[24] The existence of these bridging ligands reflects the electronic imbalance that would otherwise be associated with Ru(1), Ru(2) and Ru(3), and Ru(4) and Ru(5) in their absence. Ru(5) has a η^5-coordinated C_5Me_5 ligand with a distance of 1.830 Å, which is transferred from an external $[Cp^*Co(CO)_2]$ complex. The interaction between the Cp^{*-} ligand and the Ru(5) atom is similar to a previous report,[16] and the corresponding positive charge is proposed to be delocalised through the cluster. The supporting argument comes from the short bond length of Ru(4)–Ru(5) [2.6363(8) Å]. Ru(1), Ru(2), Ru(3) and Ru(4) are arranged to give a distorted square plane, with mean deviation 0.21 Å from the least-square plane. This Ru_4 square is capped on one side by a μ_5-nitrido ligand, which lies above the mean plane of 1.021 Å. Apart from interacting with all four metals in the square, it also bonded to the "spiked" Ru(5) atom. The angle between the Ru(4)–Ru(5) "spiked" edge and the mean plane is 77.1°. An interesting feature is that the nitrido ligand apparently does not lie above the centroid of the square, and appears to have been pushed toward the Ru(4)–Ru(5) "spiked" edge. The Ru(4)–N(1) = 2.088(4) Å and Ru(5)–N(1) = 1.985(4) Å bond lengths are both shorter than those to the atoms Ru(1), Ru(2) and Ru(3) (Ru(1)–N(1) 2.215(4), Ru(2)–N(1) 2.178(4), Ru(3)–N(1) 2.211(4) Å). The nitrido ligand is shown to be able to reside in this unusual and less regular cavity. The metal skeleton of cluster **2** might be viewed as a square pyramid with three base–apex metal–metal edges missing, in which the Ru···Ru separations (Ru(1)–Ru(5) 3.70 Å and Ru(3)–Ru(5) 3.56 Å) represent a zero bond order. The nitrido and the quadruply bridging diphenylacetylene groups are assigned to be five- and four-electron donors, respectively, and the electron count for **2** is 76, which is four electrons less than expected (80).[25] Within the formalism of the 18-electron rule, the 76-electron cluster **2** is electronically unsaturated, and a 2-electron 3-centre bond has been proposed to delocalise among the two 17-electron and one 16-electron centres bridged by two μ-CO groups, while a double bond is proposed to localise at the "spiked" edge. Alternatively, compound **2** can be described as an edge-bridged pentagonal-bipyramidal cluster. The four Ru atoms, Ru(1)–Ru(4), together with the μ_5-N and PhC_2Ph units form the pentagonal bipyramidal structure, while the CpRu(5) fragment acts as the edge-bridging unit. The electron count for this cluster in such a consideration is 82. According to the $14n+4m+2$ rule for a *closo*-deltahedral cluster,[25] for which n represents the number of transition metals and m denotes the number of main group atoms, a pentagonal bipyramidal cluster should have 70 electrons when $m=3$. Furthermore, Mingos' capping principle[26] predicts that an edge-bridging metal fragment adds 14 valence electrons to the total electron count. Therefore, the total electron count (82) is two electrons less than expected (84). The shortage of two electrons suggests that Ru–Ru double bonds may exist in the cluster and this is consistent with the observed short bond length of 2.6363(8) Å in Ru(4)–Ru(5) bond, relative to the other four Ru–Ru bonds (an average of 2.7207 Å). Molecular orbital calculations[27] of the model $[Ru_5(CO)_8(\mu\text{-}CO)_3(\eta^5\text{-}C_5H_5)(\mu_5\text{-}N)(\mu_4\text{-}\eta^2\text{-}HC_2H)]$ indeed give the highest Wiberg bond order for Ru(4)–Ru(5) (0.199) from the NBO analysis.[28, 29] The bond orders for the other Ru–Ru bonds range from 0.08 to 0.11. Figure 2 shows the spatial plots[30] of the highest occupied (Figure 2 top) and the lowest unoccupied (Figure 2 bottom) molecular orbitals. The HOMO molecular orbital is more localised on the Ru centres of the pentagonal bipyramidal moiety. However, the LUMO is mainly localised on the bridging CpRu fragment. The LUMO also has anti-bonding character between the Ru and the Cp ligand.

The formation of **2** is believed to be the result of the coupling of fragments of **1** produced at high temperature with unfragmented molecules of **1**, together with the coordination of a Cp* ligand transferred from the external mononuclear complex. An independent experiment was found to support this idea. When **1** is heated in THF in the presence of an excess of pentamethylcyclopentadiene and 1,3-cyclohexadiene, clus-

0947-6539/01/0701-0260 $ 17.50+.50/0 *Chem. Eur. J.* **2001**, *7*, No. 1

Table 1. Spectroscopic data for clusters **1**–**6**.

	IR[a] ν(CO) [cm^{-1}]	^{1}H NMR[b] δ	^{15}N HMR[c], δ	MS[d] m/z	λ_{max}[e] [nm] ($\varepsilon \times 10^{-3}$ [dm^3 mol^{-1} cm^{-1}])
1	2095 (w), 2076 (vs), 2047 (vs), 2030 (vs), 2006 (s), 1993 (sh)	6.96 (m, 4H, phenyl) 6.80 (m, 6H, phenyl) 3.44 (s, 3H, methoxy)	341.5 (s)[f]	778 (778)	316 (6.70) 435 (5.04)
2	2059 (w), 2033 (s) 2018 (vs), 1989(w) 1962 (m), 1723 (m)	6.82 (m, 6H, phenyl) 6.41 (m, 2H, phenyl) 6.06 (m, 2H, phenyl) 1.29 (s, 15H, C_5Me_5)	381.5 (s)	1140 (1140)	320 (9.72)[g] 400 (3.74)[g]
3	2060 (w), 2035(s) 2014 (m), 2003 (vs) 1958 (s), 1949 (m)	7.37 (m, 2H, phenyl) 7.18 (m, 3H, phenyl) 5.87 (d, J_{HH} = 5.75 Hz, 1H, phenyl) 5.78 (s, 1H, alkenic proton) 5.40 (d, J_{HH} = 6.55 Hz, 1H, phenyl) 4.94 (t, J_{NH} = 54.02 Hz, 1H, NH) 4.48 (m, 1H, phenyl) 4.22 (m, 1H, phenyl) 1.67 (s, 15H, C_5Me_5) 1.60 (s, 15H, C_5Me_5)	202.9 (d, J(^{15}N,H) = 76.05 Hz)	1108 (1108)	285 (21.7) 305 (21.8) 360 (13.7) 593 (2.79)
4	2089 (s), 2082 (m) 2033 (s), 2020 (m) 2012 (vs), 2003 (m) 1981 (s), 1978 (sh) 1960 (m)	I 7.20 (m, 6H, phenyl)[h] 6.94 (m, 4H, phenyl) 3.23 (s, 3H, methoxy) 2.32 (d, J_{HH} = 7.10 Hz, 1H,CH_2) 2.08 (s, 3H, Me) 1.98 (d, J_{HH} = 7.10 Hz, 1H,CH_2) 1.95 (s, 3H, Me) 1.33 (s, 3H, Me) 1.15 (s, 3H, Me) II 7.20 (m, 6H, phenyl) 6.94 (m, 4H, phenyl) 3.02 (s, 3H, methoxy) 2.12 (d, J_{HH} = 6.57 Hz, 1H,CH_2) 2.03 (s, 6H, 2Me) 1.84 (d, J_{HH} = 6.57 Hz, 1H,CH_2) 0.97 (s, 3H, Me) 0.95 (s, 3H, Me)	199.0 (s) 193.9 (s)	884 (884)	290 (16.0)[g] 459 (4.44)
5	2093 (m), 2069 (vs) 2028 (s), 2020 (vs) 2006 (m), 2001 (m) 1731 (m)	7.20 (m, 5H, phenyl) 7.03 (m, 3H, phenyl) 6.79 (m, 2H, phenyl) 3.49 (s, 3H, methoxy)	191.1(s)	621 (621)	345 (5.86)
6	2053 (s), 2045 (s) 2024 (w), 2018 (w) 1987 (vs), 1968 (w) 1943 (w)	7.58 (m, 3H, phenyl) 7.33 (m, 2H, phenyl) 7.11 (m, 5H, phenyl) 1.53 (s, 15H, C_5Me_5)	–	1210 (1210)	–

[a] In *n*-hexane. [b] In CD_2Cl_2. [c] In $CDCl_3$, with ^{1}H decoupled except for cluster **3**. [d] Calculated values in parentheses. [e] Measured in CH_2Cl_2 at 298 K. [f] From ref. [10]. [g] Shoulder. [h] Recorded at room temperature.

Table 2. Selected bond lengths [Å] and angles [°] for cluster **2**.

Ru(1)–Ru(2)	2.6926(9)	Ru(1)–Ru(4)	2.7701(7)	Ru(1)–N(1)	2.215(4)
Ru(1)–C(12)	2.352(5)	Ru(1)–C(13)	2.452(5)	Ru(2)–Ru(3)	2.6814(7)
Ru(2)–N(1)	2.178(4)	Ru(2)–C(12)	2.243(6)	Ru(3)–Ru(4)	2.7387(7)
Ru(3)–N(1)	2.211(4)	Ru(3)–C(12)	2.329(6)	Ru(3)–C(13)	2.399(6)
Ru(4)–Ru(5)	2.6363(8)	Ru(4)–N(1)	2.088(4)	Ru(4)–C(13)	2.121(5)
Ru(5)–N(1)	1.985(4)	C(12)–C(13)	1.395(8)	Ru(5)–Cp*(c)[a]	1.830
Ru(2)-Ru(1)-Ru(4)	92.24(2)	Ru(1)-Ru(2)-Ru(3)	85.83(2)	Ru(2)-Ru(3)-Ru(4)	93.19(2)
Ru(1)-Ru(4)-Ru(3)	83.25(2)	Ru(1)-Ru(4)-Ru(5)	86.42(2)	Ru(3)-Ru(4)-Ru(5)	82.89(2)
Ru(1)-N(1)-Ru(2)	75.6(1)	Ru(1)-N(1)-Ru(3)	111.5(2)	Ru(1)-N(1)-Ru(4)	80.1(2)
Ru(1)-N(1)-Ru(5)	123.6(2)	Ru(2)-N(1)-Ru(3)	75.3(1)	Ru(2)-N(1)-Ru(4)	134.7(2)
Ru(2)-N(1)-Ru(5)	144.4(2)	Ru(3)-N(1)-Ru(4)	79.1(1)	Ru(3)-N(1)-Ru(5)	115.9(2)
Ru(4)-N(1)-Ru(5)	80.6(2)	Ru(1)-C(12)-Ru(3)	102.8(2)	Ru(2)-C(12)-C(13)	127.6(4)
Ru(1)-C(13)-Ru(3)	97.9(2)	Ru(4)-C(13)-C(12)	123.6(4)		

[a] Cp*(c) denotes the centroid of the C_5Me_5 ring.

ter **2** is obtained in 4% yield (Scheme 1). Without 1,3-cyclohexadiene, there is no observable reaction under similar conditions, thus 1,3-cyclohexadiene is important and acts as a hydrogen acceptor. Hence it is believed that in both synthetic methods (involving [Cp*Co(CO)$_2$] or Cp*H), the pentamethylcyclopentadiene is transferred as a Cp*$^-$ anion.

Cluster [$Ru_3Co_2(CO)_7(\mu_3$-CO)(η^5-$C_5Me_5)_2(\mu_3$-NH){μ_4-η^8-$C_6H_4C(H)C(Ph)$}] (**3**) was found to be a Ru_3Co_2 mixed-metal imido cluster and its mass spectrum is easily interpreted. A parent peak is observed at m/z 1108, followed by the loss of eight carbonyl groups in succession. Thereafter, two envelopes corresponding to the loss of one (or two) more cyclopentadiene ring(s) are also observed. The ^{1}H NMR spectrum of **3** in CD_2Cl_2 is somewhat complicated. Apart from signals in the aromatic and aliphatic regions (with an integral

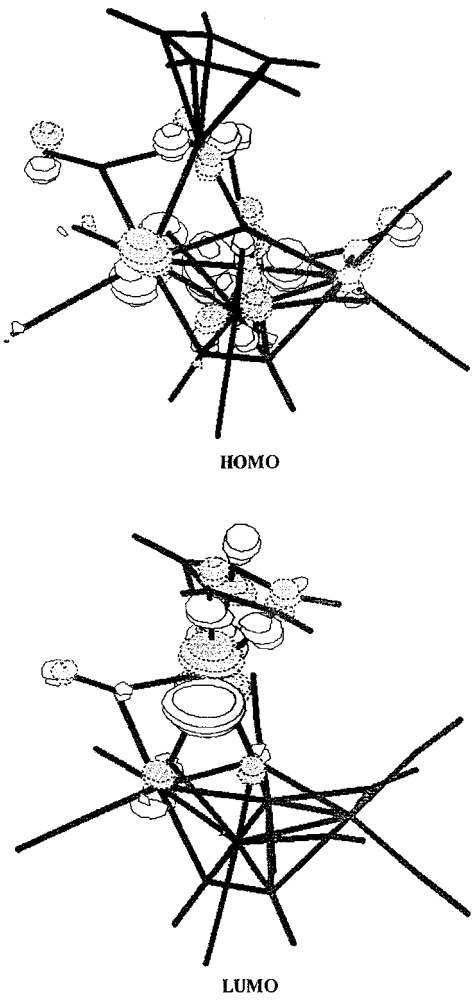

Figure 2. The spatial plots of the highest occupied (top) and the lowest unoccupied (bottom) molecular orbitals for $[Ru_5(CO)_8(\mu\text{-}CO)_3(\eta^5\text{-}C_5H_5)(\mu_5\text{-}N)(\mu_4\text{-}\eta^2\text{-}HC_2H)]$.

ratio 5:30), six resonances of equal relative intensity are observed in the range of $\delta = 4.22 - 5.87$. Of the six signals a singlet at $\delta = 5.78$ and a triplet centred at $\delta = 4.94$, with a coupling constant of 54.02 Hz are unambiguously assigned to the alkenic proton and the NH proton, respectively. Detailed assignments of the protons on the diphenylacetylene ligand were made possible with the aid of two-dimensional HH-COSY NMR spectroscopy, see Table 1 and Scheme 1. The resonances for the remaining four phenyl protons were showed to be arranged in the order $\delta = 5.87$, 4.22, 4.48 and 5.40.

Green crystals of **3**, suitable for diffraction studies, were grown from a saturated solution of $CHCl_3$/toluene at $-20\,^{\circ}C$. The molecular structure of **3** is depicted in Figure 3 and relevant structural parameters are stated in Table 3. One and a half molecules of C_7H_8, as solvent of crystallisation, were revealed in the asymmetric unit. Cluster **3** has a triangular Ru_2Co–imido structure linked to a ruthenium–cobaltocene through the $\mu_4\text{-}\eta^8\text{-}C_6H_4C(H)C(Ph)$ ligand. The imido ligand caps the Ru_2Co metal core through the coordination of the nitrogen atom (Ru(1)–N(1) 2.066(5), Ru(2)–N(1) 2.016(5) and Co(1)–N(1) 1.862(4) Å). The Ru(1)–Ru(2) and Ru(1)/Ru(2)–Co_{ave} metal–metal bond lengths of 2.7820(7) and 2.5901(9) Å, respectively, are significantly shorter than the corresponding values of 2.8555 Å[23] and 2.618 Å[31] found for $[Ru_3(CO)_{12}]$ and $[Ru_3Co(CO)_{13}]^-$. The imido nitrogen atom exhibits a doublet ($\delta = 202.9$, $J(^{15}N,H) = 76.05$ Hz) in its ^{15}N NMR spectrum. This signal is significantly downfield relative to those of $[Ru_2Co(CO)_6(\mu_3\text{-}CO)(\eta^5\text{-}C_5Me_5)(\mu_3\text{-}NH)]$[16] ($^{15}N$: $\delta = 131.4$ (d, $J(^{15}N,H) = 76.95$ Hz)); the "linked" RuCo ligand fragment is shown to be more electron withdrawing than the two carbonyl ligands. The μ_3-capping C(3)–O(3) ligand on the opposite side of the imido ligand is found to be placed towards Co(1) with a bond length of 1.897(7) Å, while Ru(1)–C(3) and Ru(2)–C(3) are equal to 2.257(6) and 2.337(7) Å, respectively. The "linked" RuCo-ligand fragment takes the place of two radial CO ligands with respect to the known complex $[Ru_2Co(CO)_6(\mu_3\text{-}CO)(\eta^5\text{-}C_5Me_5)(\mu_3\text{-}NH)]$,[16] bonding through the π interaction of carbon atoms of the phenyl group (the *ipso*-C atom is not involved). The C_4 array, which involves the remaining *ortho*- and *ipso*-carbon atoms in the ring and acetylenic carbons, is bound to Co(2) (also carrying a Cp* ligand), while C(19) and C(26) chelate Ru(3) to give a metallacyclopentadiene ring. This is the first time that this novel RuCo moiety has been reported. Complexes with metallocene moieties involving diiridium,[32] dicobalt[33] and diruthenium[34] have been reported. In previous studies, metallocyclic rings were formed by coupling of alkynes,[35–37] dialkynes[38, 39] and ynamines,[40] whereas the Ru(3)C(19)-C(24)C(25)C(26) ring in **3** is obtained by the reduction of coordinated acetylene ligand in the parent cluster **1**. The two phenyl rings are now in a *trans* configuration and the dihedral angle between the rings is equal to 32.06°. The utilisation of atoms C(20) to C(23) in binding to Ru(2) and Ru(1) destroys the aromaticity of the 1,2-C_6H_4 system. There is a localisation of π electron density as indicated by alternating long and short C–C bonds around the coordinated atoms (C(19)–C(20) 1.473(8), C(20)–C(21) 1.449(8), C(21)–C(22) 1.463(9), C(22)–C(23) 1.393(8), C(23)–C(24) 1.500(8) and C(24)–C(19) 1.446(8) Å). No such alternation occurs in the other six-membered ring, defined by C(27)–C(32), in which the C–C bond lengths only range from 1.37(1) through 1.413(9) Å, averaging 1.391 Å. The μ_3-NH proton experiences a shielding effect as it is situated above the plane of the C(19)–C(24) double bond and resonates at a significantly lower frequency of $\delta = 4.94$ than that found in $[Ru_2Co(CO)_6(\mu_3\text{-}CO)(\eta^5\text{-}C_5Me_5)(\mu_3\text{-}NH)]$ ($\delta = 7.46$, $J(N,H) = 54.80$ Hz)[16]. The Ru(3)–Co(2) bond (2.6105(9) Å) is bridged by the $C_6H_4C(H)C(Ph)$ group, with C(19) and C(26) σ-bonded to the Ru(3) atom (Ru(3)–C(19) 2.129(6), Ru(3)–C(26) 2.104(6) Å) as part of the metallacyclopentadiene ring. Three terminal carbonyls are also attached to Ru(3). A metal–metal bond completes the coordination of this ruthenium atom, which has a distorted octahedral geometry. The Co(2) atom is π-bonded to a pentamethylcyclopentadienyl ring and also to the four atoms (C(19), C(24), C(25), C(26)) of the ruthenacyclopentadienyl ring. The two rings are in a *eclipse* configuration with respect to one another. The separation between the Co(2) atom and the atoms of the C(19)C(24)C(25)C(26) ring are not equal. The Co(2)–C(19)/C(26) bond lengths (2.109(5) and 2.132(6) Å) are slightly longer than those found

0947-6539/01/0701-0262 $ 17.50+.50/0 *Chem. Eur. J.* **2001**, *7*, No. 1

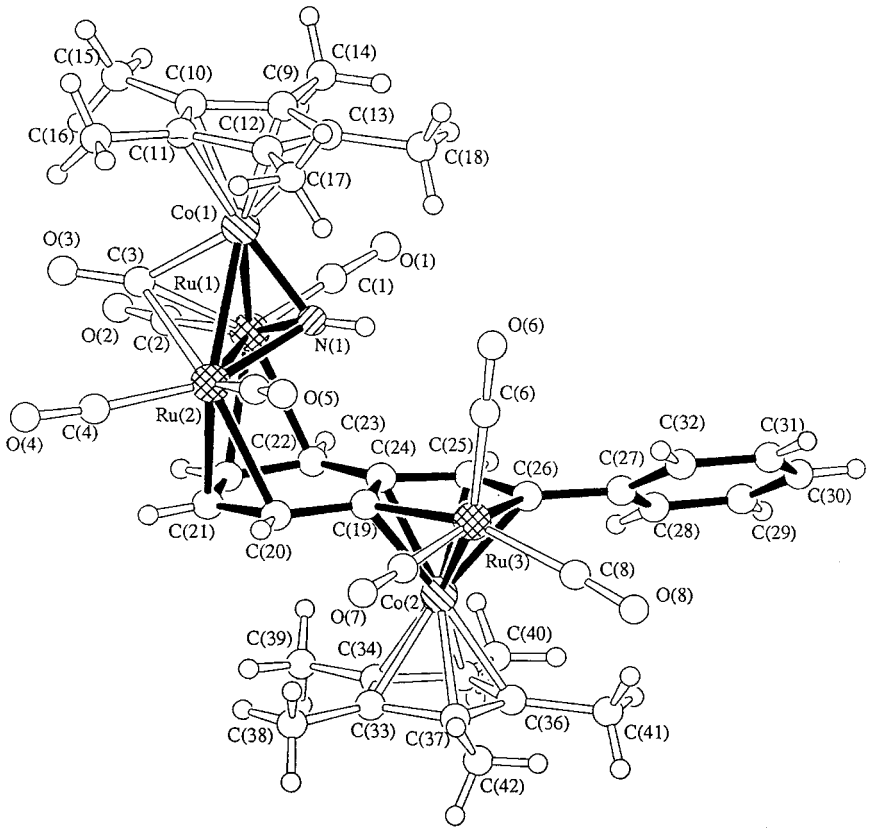

Figure 3. The molecular structure of $[Ru_3Co_2(CO)_7(\mu_3\text{-}CO)(\eta^5\text{-}C_5Me_5)_2(\mu_3\text{-}NH)\{\mu_4\text{-}\eta^8\text{-}C_6H_4C(H)C(Ph)\}]$ (**3**) with the atom numbering scheme.

Table 3. Selected bond lengths [Å] and angles [°] for cluster **3**.

Ru(1)–Ru(2)	2.7820(7)	Ru(1)–Co(1)	2.5827(9)	Ru(1)–N(1)	2.066(5)
Ru(1)–C(22)	2.311(6)	Ru(1)–C(23)	2.304(5)	Ru(2)–Co(1)	2.5974(9)
Ru(2)–N(1)	2.016(5)	Ru(2)–C(20)	2.334(5)	Ru(2)–C(21)	2.307(6)
Ru(3)–Co(2)	2.6105(9)	Ru(3)–C(19)	2.129(6)	Ru(3)–C(26)	2.104(6)
Co(1)–N(1)	1.862(4)	Co(2)–C(19)	2.109(5)	Co(2)–C(24)	2.105(5)
Co(2)–C(25)	2.065(6)	Co(2)–C(26)	2.132(6)	C(19)–C(20)	1.473(8)
C(19)–C(24)	1.446(8)	C(20)–C(21)	1.449(8)	C(21)–C(22)	1.463(9)
C(22)–C(23)	1.393(8)	C(23)–C(24)	1.500(8)	C(24)–C(25)	1.431(7)
C(25)–C(26)	1.442(8)	N(1)–H	0.87	Co(1)–Cp*(c)[a]	1.686
Co(2)–Cp*(c)[a]	1.679				
Ru(2)-Ru(1)-Co(1)	57.77(2)	Ru(2)-Ru(1)-C(22)	72.8(2)	Ru(2)-Ru(1)-C(23)	90.2(2)
C(22)-Ru(1)-C(23)	35.1(2)	Ru(1)-Ru(2)-Co(1)	57.26(2)	Ru(1)-Ru(2)-C(20)	92.9(1)
Ru(1)-Ru(2)-C(21)	74.0(2)	C(20)-Ru(2)-C(21)	36.4(2)	C(19)-Ru(3)-C(26)	77.0(2)
Ru(1)-Co(1)-Ru(2)	64.97(2)	Ru(1)-N(1)-Ru(2)	85.9(2)	Ru(1)-N(1)-Co(1)	82.1(2)
Ru(2)-N(1)-Co(1)	84.0(2)	Ru(3)-C(19)-C(24)	117.2(4)	C(19)-C(24)-C(25)	112.6(5)
C(24)-C(25)-C(26)	116.6(5)	Ru(3)-C(26)-C(25)	116.2(4)		

[a] Cp*(c) denotes the centroid of the C_5Me_5 rings.

for the inner carbons (Co(2)–C(24)/C(25) 2.105(5) and 2.065(6) Å). The perpendicular distance of Co(2) from the plane of the ruthenacyclopentadienyl fragment is 1.678 Å, which is very similar to the distance from the Cp* ring (1.679 Å). This ruthenacyclopentadienyl ring consists of two slightly longer bonds (C(19)–C(24) 1.446(8), C(25)–C(26) 1.442(8) Å) and one shorter C–C bond (C(24)–C(25) 1.431(7) Å), which is an intermediate value between a C–C single and C=C double bond length; this is consistent with considerable back bonding from Co(2) to the metallocyclic ring. The bond angles within the ring are nearly 120°, and thus this metallocyclic system can be viewed as somewhat delocalised diene. The planes of the 1,2-C_6H_4 phenyl and ruthenacyclic rings are essentially coplanar, with a mean deviation of 0.0477 Å. The pentamethylcyclopentadienyl rings bonded to Co(1) and Co(2) are almost parallel to this central plane; the dihedral angles are 7.27° and 4.65°, respectively. And the angle between the Cp* rings is 2.63°. The bonding between the μ_4-η^8-$C_6H_4C(H)C(Ph)$ fragment and the cluster is attained through σ bonds of Ru(3) with C(19) and C(26) and a donation of the eight π-electrons of the C_6H_4 and metallacyclic rings to Ru(1), Ru(2) and Co(2). Thus the μ_4-η^8-$C_6H_4C(H)C(Ph)$ moiety donates a total of ten electrons to the whole cluster system. If we consider the μ_3-NH imido fragment as a four-electron donor, a total of 82 cluster valence electrons results. This is consistent with the sum of valence electrons required of dinuclear and trinuclear systems.

Another new compound isolated in this reaction is $[Ru_3(CO)_7(\mu\text{-}\eta^6\text{-}C_5Me_4CH_2)\{\mu\text{-}\eta^3\text{-}PhC_2(Ph)C(O)N(OMe)\}]$ (**4**). The spectroscopic data of **4** are presented in Table 1. Its IR spectrum shows the presence of CO stretching frequencies of terminal carbonyls only. The mass spectrum exhibits a molecular ion envelope that agrees with the formulation proposed, with ion peaks corresponding to CO losses. Two absorption bands are displayed at 290 and 459 nm in the UV-visible spectrum of **4**. The ^1H and ^{15}N NMR spectra of **4** are rather complex. Other than the resonances in the aromatic region in the ^1H NMR spectrum of **4**, there are nine singlets and four doublets present in the range of $\delta = 3.23$ to 0.95, which are significantly more than expected. The ^{15}N NMR studies of ^{15}N-enriched samples of **4** gave two singlets at $\delta = 199.0$ and 193.9. In order to establish the molecular structure of **4**, the compound was characterised by X-ray crystallographic analysis (Figure 4). Selected bond parameters are given in Table 4. Cluster **4** is a metallapyrrolidone cluster with an open trimetallic core, and such a skeleton is unprecedented. The three ruthenium atoms are joined by Ru–Ru single bonds (Ru(1)–Ru(2) 2.937(1) and Ru(2)–Ru(3) 2.698(1) Å) with an

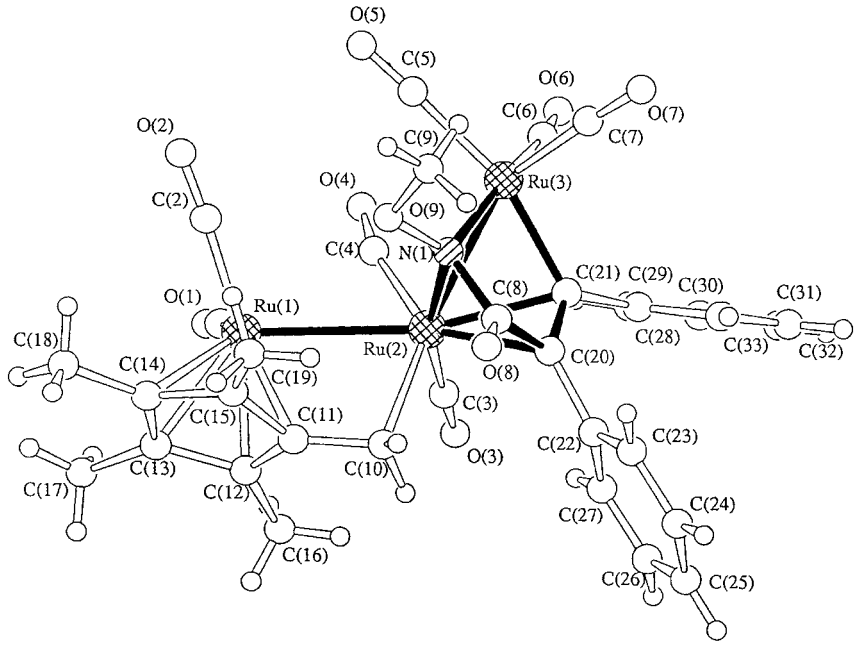

Figure 4. The molecular structure of $[Ru_3(CO)_7(\mu\text{-}\eta^6\text{-}C_5Me_4CH_2)\{\mu\text{-}\eta^3\text{-}PhC_2(Ph)C(O)N(OMe)\}]$ (**4**) with the atom numbering scheme.

Table 4. Selected bond lengths [Å] and angles [°] for cluster **4.**

Ru(1)–Ru(2)	2.937(1)	Ru(2)–Ru(3)	2.698(1)	Ru(2)–N(1)	2.215(7)
Ru(2)–C(10)	2.24(1)	Ru(2)–C(20)	2.294(9)	Ru(2)–C(21)	2.263(9)
Ru(3)–N(1)	2.068(8)	Ru(3)–C(21)	2.061(10)	O(9)–N(1)	1.421(10)
O(8)–C(8)	1.22(1)	O(9)–C(9)	1.44(1)	N(1)–C(8)	1.41(1)
C(8)–C(20)	1.48(1)	C(10)–C(11)	1.41(1)	C(20)–C(21)	1.42(1)
Ru(1)–Cp*(c)[a]	1.8778				
Ru(1)-Ru(2)-Ru(3)	118.22(4)	Ru(1)-Ru(2)-N(1)	105.1(2)	Ru(1)-Ru(2)-C(10)	73.9(3)
Ru(1)-Ru(2)-C(20)	152.7(3)	Ru(1)-Ru(2)-C(21)	165.9(2)	Ru(3)-Ru(2)-N(1)	48.6(2)
Ru(3)-Ru(2)-C(10)	144.7(3)	Ru(2)-Ru(3)-N(1)	53.4(2)	N(1)-Ru(3)-C(21)	76.0(4)
N(1)-O(9)-C(9)	110.7(7)	Ru(2)-N(1)-Ru(3)	78.0(3)	Ru(2)-N(1)-O(9)	129.1(5)
Ru(3)-N(1)-O(9)	121.2(6)	Ru(3)-N(1)-C(8)	118.1(6)	N(1)-C(8)-C(20)	105.9(9)
Ru(2)-C(10)-C(11)	102.4(7)	Ru(1)-C(11)-C(10)	117.3(7)	C(8)-C(20)-C(21)	115.2(9)
Ru(3)-C(21)-C(20)	116.0(7)				

[a] Cp*(c) denotes the centroid of the C_5Me_5 ring.

opening angle of 118.22(4)° and are bridged by the μ-η^6-tetramethylfulvene and the μ-η^3-$PhC_2(Ph)C(O)N(OMe)$ ligands. Ru(1) adopts a distorted "piano stool" coordination geometry. One of the methyl groups of the Cp* ligand has undergone a C–H bond activation and transforms into a CH_2 group, which forms a σ-bond with Ru(2), thus producing a four-membered ring that contains the C(10) and C(11) carbon atoms of the Cp* ring and the Ru(1) and Ru(2) atoms of the cluster. The carbon atoms of all methyl groups are displaced from the average plane of the five-membered ring (which is planar within 0.0153 Å) in the direction opposite to the Ru(1) atom. In contrast, the C(10), which belongs to the methylene group σ-bonded to the Ru(2) atom, is displaced from the Cp-ring plane by 0.123 Å in the direction of the Ru(1) atom. The inclination angle of the C(10)–C(11) vector to the Cp-ring plane in **4** is 6.3°. This C_5 plane is 1.878 Å from the Ru(1) atom. The distance between Ru(2) and the *exo*-methylene carbon C(10) is 2.24(1) Å, which is similar to the 2.240(9) Å found in $[Ru_6(CO)_{14}(\mu\text{-}\eta^1\text{:}\eta^5\text{-}C_5Me_4CH_2)(\mu_6\text{-}C)]$[41] and the 2.204(10) Å in $[Ru_6(CO)_{14}(\mu\text{-}\sigma\text{:}\eta^5\text{-}C_5H_4CH_2)]$.[42] The Ru(2)-C(10)-C(11) angle (102.4(7)°) is close to the theoretically expected valence angle for a sp^3 carbon (109.5°). These features are all consistent with the following coordination mode of the tetramethylfulvene ligand: the five-membered ring of the fulvene ligand is bound to the $Ru(CO)_2$ fragment in η^5 fashion, while the *exo*-methylene part is bound to Ru(2) in η^1 fashion. It is believed that the Ru(2)–CH_2 bond is essentially a single σ bond, with no significant contribution from the olefinic structure as observed in the complex $[(\eta^5\text{-}C_5Me_5)(\eta^6\text{-}C_5Me_4CH_2)TiCH_2]$.[43] The Ru(1)–C(10) and Ru(1)–C(11) bond lengths of of 2.90 Å and 2.26(1) Å, respectively, indicate that there is no interaction between the methylene group and Ru(1). It should be noted, however, that the bond between the *exo*-methylene carbon and a ring carbon (C(10)–C(11) 1.41(1) Å) is somewhat shorter than the other four C–C(Me) single bonds projecting out of the five-membered ring. This fact can be interpreted as a sign of the remaining double-bond character on the C(10)–C(11) bond of the fulvene ligand. The disposition of the C_5 ring and the *exocyclic* CH_2 arm is similar to that encountered in $[Ru_6(CO)_{14}(\mu\text{-}\eta^1\text{-}\eta^5\text{-}C_5Me_4CH_2)(\mu_6\text{-}C)]$,[41] which has been isolated from the thermolysis of $[Ru_6(CO)_{17}(\mu_6\text{-}C)]$ with C_5Me_5H. Thermolysis of **4** with a slight excess of $[Ru_3(CO)_{12}]$ in *n*-octane gives the known $[Ru_6(\mu_3\text{-}H)(CO)_{12}(\mu\text{-}CO)(\mu_4\text{-}\eta^2\text{-}CO)_2(\eta^5\text{-}C_5Me_5)]$[44] cluster in low yield. Apart from the tetramethylfulvene ligand, Ru(2)–Ru(3) (2.698(1) Å) is bridged by the μ-η^3-$PhC_2(Ph)C(O)N(OMe)$ ligand, which is derived from the coupling of the nitrene ligand, CO and the acetylene ligand in starting cluster **1**. This flyover-type ligand is coordinated to ruthenium atoms through N(1), C(20) and C(21) and is attached to Ru(3) through a σ bond from C(21) and a dative bond from N(1). The bonding to Ru(2) involves a π interaction with C(20)=C(21) and a σ bond from N(1). The coupling of the μ_3-NOMe ligand with another fragment, CO and PhC_2Ph in this case, is rather rare, and the only example we are aware of is $[Ru_2(CO)_6\{\mu\text{-}\eta^3\text{-}HC_2(Ph)C(O)N(OMe)\}]$.[10] The metallapyrrolidone ring system involving Ru(3), N(1), C(8), C(20) and C(21) is essentially planar, with

0947-6539/01/0701-0264 $ 17.50+.50/0 *Chem. Eur. J.* **2001**, *7*, No. 1

maximum deviations of 0.2615 Å from planarity associated with C(8), and the Ru(2) atom is found to lie at 1.965 Å from this pentagonal base plane. The metallapyrrolidone carbonyl is not bonded to either metal atom, whereas the nitrogen atom bridges both metals asymmetrically. The dative bond to Ru(3) is significantly shorter (2.068(8) Å) than the σ bond to Ru(2) (2.215(7) Å). As a consequence of these N–Ru interactions and the coupling of N(1) to C(8), there should be a single-bond interaction between N(1) and O(9) (bond length 1.421(10) Å). Nevertheless, this N(1)–O(9) bond is shorter than that of the starting cluster **1** (1.453(4) Å).[10] The solution structure of **4** is more complicated than its solid-state structure, as evidenced by the ^{1}H and ^{15}N NMR studies. One may suspect the presence of isomerisation or a rearrangement process in solution. This assumption was supported by the variable-temperature ^{1}H NMR study of cluster **4**. Upon an increase in the temperature from 213 to 293 K, two sets of signals are distinguished, with the integral ratio gradually changing from 1:1.62 to 1:1.17 and no broadening or coalescence of signals being observed. The singlets at $\delta =$ 3.23 and 3.02 are assigned to the methoxy groups of each isomer. The sharp signal of the C_5Me_5 ligand is now replaced by four magnetically nonequivalent methyl signals at $\delta = 2.08$, 1.95, 1.33 and 1.15 for isomer I and $\delta = 2.03$, 0.97 and 0.95 for isomer II, and two doublets at $\delta = 2.32$ and 1.98 (J_{gem}(H,H) = 7.10 Hz) for I and $\delta = 2.12$ and 1.84 (J_{gem}(H,H) = 6.57 Hz) for II, due to an *exocyclic* CH_2 group.

To establish the exchange process of the two isomers, the two-dimensional EXSY ^{1}H NMR experiment was performed at 298 K in CD_2Cl_2, as shown in Figure 5, with a mixing time of 100 ms. Strong magnetization transfer peaks were observed between the resonances of the two isomers. All the ^{1}H NMR signals are shown to exchange pairwise. On the basis of the above-reported assignment, the pairwise exchanges (for the protons other than the phenyl groups) that take place are summarised in Table 5. The magnetization transfer indicates that there is a facile isomerisation between the two forms. There is no basis for specifically assigning the individual exchange of phenyl protons in the two isomers. The nature of isomerisation is not clear although one may suggest that some restriction in the rotation of this N–O bond is present and leads to two isomers of **4**. However, the energy barrier for conversion is rather large and is not in agreement with conformational change due to simple N–O bond rotation. An alternative way to give isomeric forms of **4** is the flipping of the four-membered ring defined by Ru(1), Ru(2), C(10) and the centroid of Cp* (maximum deviation 0.08 Å), but there is no strong evidence to support this process.

The carbons that originated in the coordinated alkyne are bonded to the Ru(2)–Ru(3) edge as a σ,π-vinyl ligand. The C(20)–C(21) distance within the ligand is 1.42(1) Å, typical of a π-bonded olefin ligand and corresponding to a bond order of 1–2. It is noteworthy that this organic ligand also contributes six electrons to the core, the same as the μ-η^6-tetramethylfulvene fragment when regarding the dative bond from N(1) and the η^2-coordinated olefin as two-electron donors and the σ-bonded N and C atoms as one-electron donors.

Crystallisation of the pale yellow band gave yellow crystals of **5**, formulated as [$Ru_2(CO)_6$\{μ-η^3-PhC_2(Ph)C(O)N(OMe)\}] from its mass spectrum. (Table 1) The ^{1}H and ^{15}N NMR spectra confirm the presence of organic groups. Furthermore, other than characteristic absorptions of terminal carbonyl

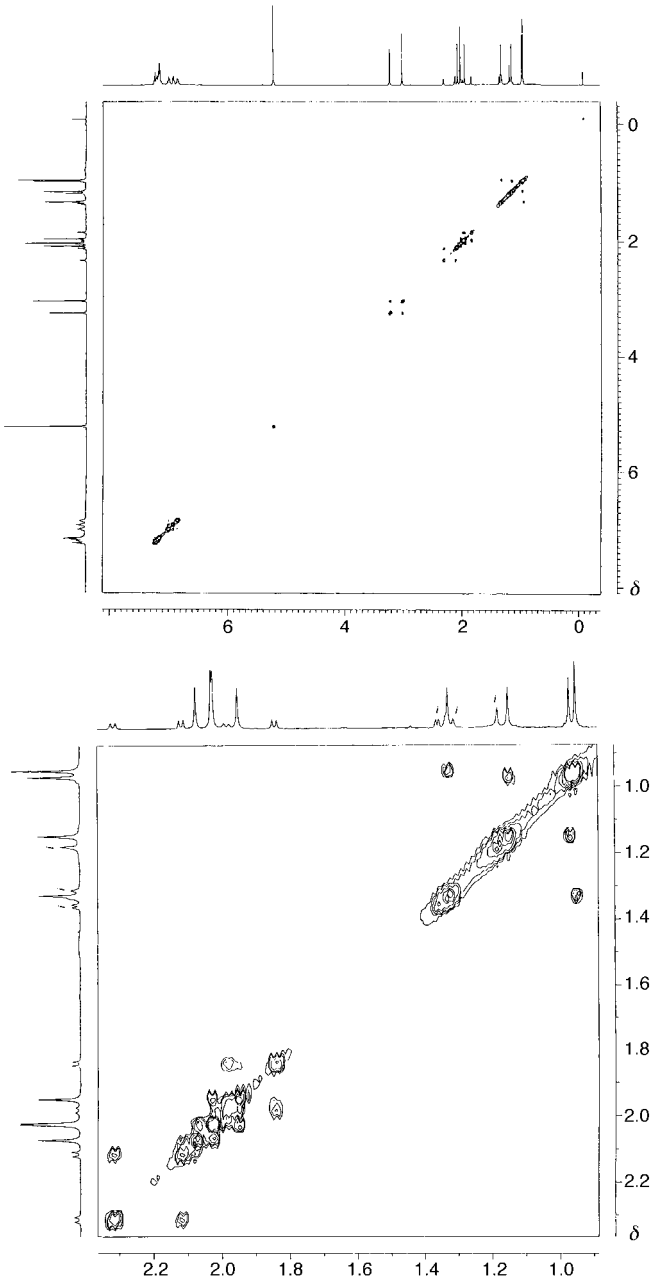

Figure 5. Contour plot of a two-dimensional EXSY ^{1}H NMR experiment for **4** in CD_2Cl_2 at 298 K. The mixing time was 100 ms. Full spectrum (top) and expanded spectrum (bottom) of selected region. *i* indicates impurities.

Table 5. The assignment of the pairwise exchanges for the protons other than those on the phenyl groups of isomers I and II of cluster **4**.

I δ		II δ	Assignment
3.23	↔	3.02	methoxy
2.32	↔	2.12	methylene proton
2.08	↔	2.03	methyl
1.98	↔	1.84	methylene proton
1.95	↔	2.03	methyl
1.33	↔	0.95	methyl
1.15	↔	0.97	methyl

groups, the infrared spectrum in the ν(CO) stretching region has a weak band at 1731 cm^{-1}, which could be attributed to a ketonic carbonyl group. The spectroscopic data of **5** indicate its structure to be analogous to the crystallographically determined $[Ru_2(CO)_6\{\mu\text{-}\eta^3\text{-}HC_2(Ph)C(O)N(OMe)\}]$.[10] They displayed similar IR spectra, particularly the ν(CO) band present in the carbonyl group of the metallacycle. All the other complexes isolated in this reaction are known compounds and were identified by a comparison of their spectroscopic data with those reported.

Reaction of $[Ru_3(CO)_9(\mu_3\text{-}NOMe)(\mu_3\text{-}\eta^2\text{-}PhC_2Ph)]$ (1) with $[Cp^*Co(CO)I_2]$: Heating complex **1** with $[Cp^*Co(CO)I_2]$ under reflux in THF for 2 hours afforded a dark brown solution. A new mixed-metal carbonyl cluster $[Ru_3Co(CO)_5(\eta^5\text{-}C_5Me_5)(\mu_4\text{-}N)(\mu_3\text{-}\eta^2\text{-}PhC_2Ph)(\mu\text{-}I)_2I]$ (**6**) was isolated in low yield (Scheme 2). It was characterised by various spectroscopic methods (Table 1) and its structure was also established by single-crystal X-ray crystallography. Cluster **6** contains a distorted Ru_3Co butterfly skeleton with a nitrido ligand bonded to all four metal centres and with a Ru–Ru wing-edge found to be missing. Its IR spectrum reveals only terminal carbonyl ligand activity. The positive FAB mass spectrum displayed a molecular ion peak at m/z 1210 and daughter ions due to successive loss of carbonyls. In the ^1H NMR spectrum, apart from the singlet due to the Cp* ligand, there are multiplets in the aromatic region, with an integration of ten protons compared to Cp* (15 protons). Unfortunately, the extremely poor yield of **6** precludes any satisfactory ^{15}N NMR measurements.

The molecular structure of the tetranuclear mixed-metal nitrido cluster **6** is shown in Figure 6, with selected interatomic distances and angles summarised in Table 6. In the solid state, the four metal atoms in **6** define a distorted butterfly geometry less one wing-edge Ru–Ru bond. A similar Ru_3Co metal skeleton has previously been observed.[16] The Cp*Co unit is at one of the wing-tips of the butterfly, opposite to the iodide groups which bridge the Ru(1)···Ru(2) and Ru(2)–Ru(3) wing edges; the third iodine atom is terminally coordinated to an equatorial site of the Ru(3) atom. A μ_3-

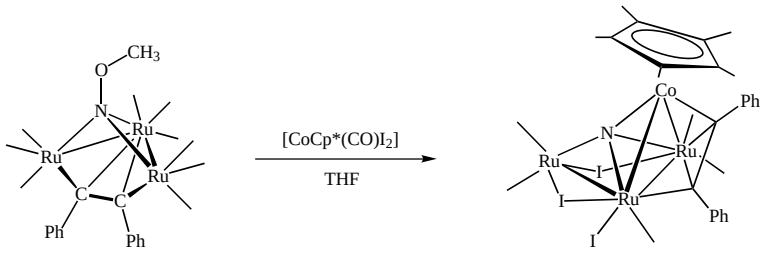

1 **6**

Scheme 2. Reaction of cluster **1** with two equivalents of $[Cp^*Co(CO)I_2]$ afforded cluster complex **6** in low yield.

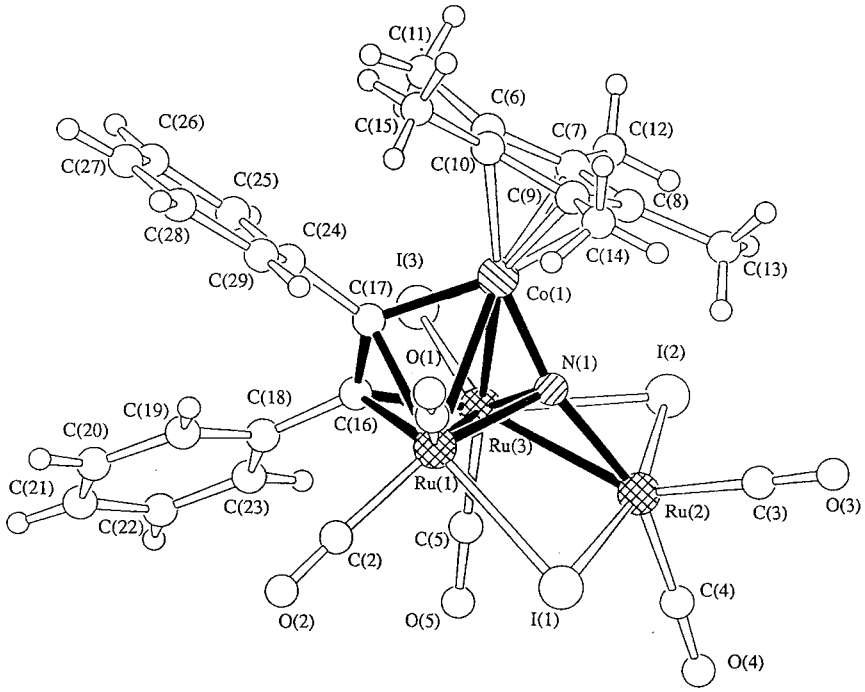

Figure 6. The molecular structure of $[Ru_3Co(CO)_5(\mu^5\text{-}C_5Me_5)(\mu_4\text{-}N)(\mu_3\text{-}\eta^2\text{-}PhC_2Ph)(\mu\text{-}I)_2I]$ (**6**) with the atom numbering scheme.

Table 6. Selected bond lengths [Å] and angles [°] for cluster **6**.

I(1)–Ru(1)	2.733(2)	I(1)–Ru(2)	2.689(2)	I(2)–Ru(2)	2.654(2)
I(2)–Ru(3)	2.874(2)	I(3)–Ru(3)	2.703(2)	Ru(1)–Ru(3)	2.751(2)
Ru(1)–Co(1)	2.650(2)	Ru(1)–N(1)	2.06(1)	Ru(1)–C(16)	2.23(1)
Ru(1)–C(17)	2.22(1)	Ru(2)–Ru(3)	2.779(2)	Ru(2)–N(1)	2.037(10)
Ru(3)–Co(1)	2.767(2)	Ru(3)–N(1)	1.98(1)	Ru(3)–C(16)	2.01(1)
Co(1)–N(1)	1.79(1)	Co(1)–C(17)	1.97(1)	C(16)–C(17)	1.39(2)
Co(1)–Cp*(c)[a]	1.726				
Ru(1)-I(1)-Ru(3)	75.58(4)	Ru(2)-I(2)-Ru(3)	60.20(4)	Ru(3)-Ru(1)-Co(1)	61.61(5)
C(16)-Ru(1)-C(17)	36.4(5)	I(1)-Ru(2)-I(2)	164.43(6)	I(2)-Ru(3)-I(3)	88.29(5)
Ru(1)-Ru(3)-Ru(2)	73.85(4)	Ru(1)-Ru(3)-Co(1)	57.40(5)	Ru(2)-Ru(3)-Co(1)	86.28(5)
Ru(1)-Co(1)-Ru(3)	60.99(5)	Ru(1)-N(1)-Ru(2)	108.6(5)	Ru(1)-N(1)-Ru(3)	85.8(4)
Ru(1)-N(1)-Co(1)	86.8(4)	Ru(2)-N(1)-Ru(3)	87.4(4)	Ru(2)-N(1)-Co(1)	164.6(6)
Ru(3)-N(1)-Co(1)	94.2(5)	Ru(1)-C(16)-Ru(3)	80.9(5)	Ru(1)-C(16)-C(17)	71.4(8)
Ru(3)-C(16)-C(17)	103.8(9)	Ru(1)-C(17)-Co(1)	78.4(5)	Co(1)-C(17)-C(16)	116.6(10)

[a] Cp*(c) denotes the centroid of the C_5Me_5 ring.

0947-6539/01/0701-0266 $ 17.50+.50/0 *Chem. Eur. J.* **2001**, *7*, No. 1

η^2-PhC_2Ph ligand caps the Ru_2Co wing face. The centroid of the Cp* ligand is found to be 1.726 Å from Co(1). The metal–metal bond lengths in **6** are in the range of 2.650(2) to 2.779(2) Å. The Ru(1)···Ru(2) separation (3.32 Å) represents a zero bond order, which is bridged by a three-electron μ-I group. The nitrido N atom is asymmetrically bonded to the four metal atoms (bond length range 1.79(1)–2.06(1) Å), with the nitrido atom tilted towards Co(1). The Ru(1)-N(1)-Ru(3) and Ru(2)-N(1)-Co(1) angles are found to be 85.8(4) and 164.6(6)° respectively, both of which deviate from those found in the "real" butterfly cluster, $[Ru_3Co(\mu\text{-H})(CO)_9(\eta^5\text{-}C_5Me_5)(\mu_4\text{-N})]$ (Ru(1)-N(1)-Ru(3) 83.1(1) and Ru(2)-N(1)-Co(1) 175.0(2)°).[16] The alkyne ligand is bound to the Ru_2Co triangular face in the common μ_3-η^2-$\parallel$ bonding mode, with the C–C bond parallel to the Ru(3)–Co(1) wing edge and offset towards Ru(1). The $M–C_{alkyne}$ bond lengths may be divided into two groups: two long bonds to Ru(1) atom (Ru(1)–C(16) 2.23(1) and Ru(1)–C(17) 2.22(1) Å) and two short ones (Ru(3)–C(16) 2.01(1) and Co(1)–C(17) 1.97(1) Å). The Ru(3)–Co(1) edge (2.767(2) Å) parallel to the alkyne bond is somewhat longer than the Ru(1)–Ru(3) and Ru(1)–Co(1) separations (Ru(1)–Ru(3) 2.751(2) and Ru(1)–Co(1) 2.650(2) Å). The alkyne group causes the Cp* ligand to displace below this Ru_2Co triangular plane, with a dihedral angle between planes of 79.9°. The alkyne originates from the starting Ru_3 cluster **1**, and moves to the Ru_2Co wing face in **6** with the C–C bond parallel to Ru(3)–Co(1). This orientation may be correlated with the electron-accepting properties of the three metal fragments constituting the cluster.[45] The more electron-attracting fragments appear to locate in the "basal" positions II or III, rather than in the "apical" position I, see Figure 7.

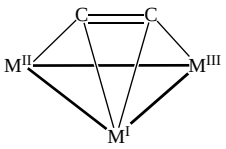

Figure 7. Labelling scheme for $M_3(\mu_3\text{-}\eta^2\text{-}C_2)$ fragment.

Model calculations indicate that the alkyne behaves as an overall donor of electron density and bonds most strongly to positions II and III, so that the more electron-accepting fragments will locate at these positions. Thus, in cluster **6**, the least electron-attracting Ru(1), with only one iodide ligand, is located in the "apical" position I, while Ru(3) with two iodides and the Cp*Co fragments occupy the "basal" positions II and III. The μ-I and the μ_3-η^2-PhC_2Ph ligands are both regarded as three- and four-electron donors, respectively,[46] hence a cluster valence electron (CVE) count of 64 results; this is consistent with a tetranuclear cluster with only four metal–metal bonds.

^{15}N NMR spectroscopy: The chemical shift in ^{15}N NMR spectroscopy is sensitive to local geometry and it is a useful tool in characterising nitrido and nitrene clusters. Upon thermolysis of **1** with $[Cp^*Co(CO)_2]$, cluster **2** was formed which exhibits a ^{15}N chemical shift at $\delta = 381.5$. The coordination mode of the μ_5-nitrido N atom in **2**, in which the five ruthenium atoms arranged as a "spiked", square-planar metal skeleton, is unprecedented. When considering cluster **2** as square pyramidal with three base-apex metal–metal edges missing, the μ_5-N atom gives an unusual upfield shift of $\delta =$ 83.4 relative to the semi-interstitial nitrogen atom in $[Ru_5(CO)_{14}(\mu_5\text{-N})]^-$ ($\delta = 464.9$).[47] Even on protonation of this anion, a decrease of only δ 27–30 is proposed to be observed in the chemical shift value.[48] Cluster **2** is strictly an outlier to the correlation, stated by Mason,[49, 50] between the shift and a compression of the interstitial (in which the interstitial shares all its valence electrons in σ and π bonding with the cluster). This considerable scatter introduced into the correlation by irregularity in the cavity produced by disposition of external capping acetylene ligand. Higher field (greater shielding at nitrogen) shifts in this unsaturated 76 electron cluster may be attributed to anisotropic effects similar to that in aromatic compounds.[51] In cluster **2**, the "spiked" ruthenium bonded to the nitrene N atom and may be viewed as a substituent to a "$\{Ru_4(CO)_{11}(\mu_4\text{-N})(\mu_4\text{-}\eta^2\text{-}PhC_2Ph)\}$" fragment. Combining the results obtained before,[10] the substituents of –H ($\delta = 47.6$, $J(^{15}N,H) = 70.54$ Hz), –C(O)OMe ($\delta = 79.9$), –OMe ($\delta = 301.6$) and –Ru ($\delta = 381.5$) modify the electronic environment and even the chemical shifts of the nitrogen atom in these clusters, according to their electron-accepting ability. The imido group in cluster **3** was found to display a doublet nitrogen resonance at $\delta = 202.9$ ($J(^{15}N,H) = 76.05$ Hz). This observed $J(^{15}N,H)$ coupling constant is fully consistent with calculated value with a deviation of only 0.38%. The $^{15}N–H$ coupling can be converted to $^{14}N–H$ coupling by the equation $J(^{14}N,H) = -0.713 \times J(^{15}N,H)$, in which -0.713 comes from γ_{14}/γ_{15}.[52] Cluster **3** is somewhat like $[Ru_2Co(CO)_6(\mu_3\text{-CO})(\eta^5\text{-}C_5Me_5)(\mu_3\text{-NH})]$ ($\delta = 131.4$, $J(^{15}N,H) = 76.95$ Hz) by further linkage to a $\{RuCo(CO)_3(\eta^5\text{-}C_5Me_5)\}$ fragment through the μ_4-η^8-$C_6H_4C(H)C(Ph)$ ligand. The coupling constant (76.05 Hz) for direct $^{15}N–H$ interaction in this μ_3-NH imido group is similar to those reported (~77 Hz).[16] Clusters **4** and **5** are both metallapyrrolidone complexes. These two clusters differ from each other by further coordination of a $\{Ru(CO)_2(\mu\text{-}\eta^6\text{-}C_5Me_4CH_2)\}$ moiety in cluster **4**. The measurements made in this study on these ruthenium clusters are the first reported for complexes that have exclusively metallapyrrolidone ligands, μ-η^3-$PhC_2(Ph)C(O)N(OMe)$. Their ^{15}N resonances are located at $\delta = 193.9$ and 199.0 for **4** and $\delta = 191.1$ for **5**; this range is found to be a clear window for a characteristic nitrogen environment. The coordination of the extra $\{Ru(CO)_2(\mu\text{-}\eta^6\text{-}C_5Me_4CH_2)\}$ fragment in **4** leads to a downfield shift of only a few ppm in its ^{15}N NMR spectrum. In the ^{1}H fully coupled ^{15}N NMR spectra, those singlets present for clusters **4** and **5** split into doublets ($\delta = 199.0$, $^3J(^{15}N,H) = 3.03$ Hz; $\delta = 193.9$, $^3J(^{15}N,H) = 3.13$ Hz; $\delta = 191.1$, $^3J(^{15}N,H) = 3.15$ Hz). The parent cluster $[Ru_3(CO)_9(\mu_3\text{-CO})(\mu_3\text{-NOMe})]$ is reported to have a $^3J(^{15}N,H)$ coupling constant of 4.4 Hz.[53] Together with the results in our previous report,[10, 16, 17] a close relationship between the cluster structure and the chemical shift of the cluster nitrogen atom in ^{15}N NMR spectra has fruitfully developed into an easy and rapid method for the analysis of the products in this system.

Electrochemistry: In order to investigate the redox properties of the compounds prepared in this study, the electrochemistry of clusters **1**, **2** and **4** has been examined in CH_2Cl_2 by using cyclic voltammetry and controlled potential coulometry, with *n*-tetrabutylammonium hexafluorophosphate (TBAHFP) as a

supporting electrolyte. The redox potential values obtained are presented in Table 7; for comparison, compound $[Ru_3(CO)_9(\mu_3\text{-}CO)(\mu_3\text{-}NOMe)]$ (**A**), which has been reported previously, is also listed.[16]

Table 7. Electrochemical data[a] for compounds **1**, **2**, **4** and $[Ru_3(CO)_9(\mu_3\text{-}CO)(\mu_3\text{-}NOMe)]$ **A**[16]

	Oxidation E_{pa} [V][b]	Reduction E_{pc} [V][b]
A	1.11	−1.66
1	1.12	−1.62
2	0.99	−1.12
4	0.76	−1.70

[a] $\sim 10^{-3}$ M cluster in 0.1M TBAHFP in dichloromethane at 298 K, the working electrode was a glassy carbon electrode, the auxiliary and the reference electrodes were a platinum wire and $Ag/AgNO_3$, respectively. Scan rate was 100 mV s^{-1}. The potentials are referenced to the $Ag/AgNO_3$ (0 V) under the same conditions, calibrated with ferrocene. [b] E_{pa} and E_{pc} are the anodic and cathodic potentials, respectively.

The parent cluster **A**, which reacts with excess diphenylacetylene to produce cluster **1**, undergoes a single, irreversible one-electron transfer step with $E_{pc} = -1.66$ V against $Ag/AgNO_3$ yielding the corresponding anion $\mathbf{A}^-$. In addition to this reduction step, cluster **A** also exhibits an irreversible anodic wave at $E_{pa} = 1.11$ V. Controlled potential coulometry at the oxidation step ($E_w = 1.25$ V) indicates that this anodic process consumes 1 faraday mol^{-1} of **A**. On the basis of the relative peak currents of the cathodic and anodic waves, the reduction process is thus assigned to be an one-electron step. The irreversibility of these processes implies cluster decomposition and further investigation was terminated. It is believed that the incorporation of an alkyne ligand in the cluster framework might lead to changes in redox behaviour. The cyclic voltammogram of compound **1** in dichloromethane contained an irreversible cathodic wave at $E_{pc} = -1.62$ V against $Ag/AgNO_3$, along with weak oxidations at -0.82 and -0.13 V. The region in which weak oxidation waves appear was initially empty, with the waves appearing after the cathodic wave was traversed. Cyclic voltammetric measurements were obtained at scan rates varying from 50 to 1000 mV s^{-1}, but the ΔE_p values remained virtually unchanged. For **1**, an additional irreversible anodic wave was located at $E_{pa} = 1.12$ V. Applying a working potential (E_w) at 1.25 V, controlled potential coulometry showed that it involves 1 faraday mol^{-1} of **1** in this oxidation step. The similarity of the relative peak heights for both couples within a given voltammogram points to the same number of electrons being involved in the oxidation and reduction of cluster **1**. One-electron accession in the cluster **1** is believed to afford the 51 electron cluster $\mathbf{1}^-$, which is unstable and loses a CO ligand to give the 49 electron species $[Ru_3(CO)_8(NOMe)(PhC_2Ph)]^-$,[54] following an EC mechanism (E = electrochemical process, C = chemical process). A well-defined reduction peak is observed for **2** at $E_{pc} = -1.12$ V. The reversal of the scan direction just after this cathodic peak is traversed leads to anodic peaks at -1.00 and -0.75 V. Controlled potential coulometric tests with respect to this cathodic process ($E_w = -1.3$ V) show that it involves the consumption of two electrons per molecule. Similarly, an irreversible two-electron reduction wave is observed in the square pyramidal cluster $[Ru_5N(CO)_{14}]^-$.[54] The analysis of the cyclic voltammetric response at scan rates varying from 50 to 1000 mV s^{-1} indicates that the process occurring at the cathodic wave, to which the reoxidation peaks are related, seems to be due to a charge transfer with a low degree of reversibility. In addition the anodic-to-cathodic peak current ratio decreases in the range from 50 to 1000 mV s^{-1}. These data are consistent with a process in which a rapid chemical reaction follows the formation of the electrogenerated species. The reoxidation daughter peaks is attributed to the oxidation of the resulting electroactive compounds (EEC/ECEC mechanism) or, alternatively, to the oxidation of a product that results from a further chemical reaction (EECC/ECECC mechanism). Besides, cluster **2** can also be oxidised, as shown by the presence of an anodic CV wave with $E_{pa} = 0.99$ V on a positive-potential scan. A weak reduction wave is observed at -0.42 V upon scan reversal. Based on the relative peak heights, the oxidative wave is tentatively assigned to the +2/0 redox couple. In comparison to the closely related clusters $[Ru_4(CO)_9(\mu\text{-}CO)_2(\mu_4\text{-}NR)(\mu_4\text{-}\eta^2\text{-}PhC_2Ph)]$ [R = OMe, H and C(O)OMe][16] which exhibit only irreversible reductions at about $E_{pc} = -1.3$ V within the solvent limits,[16] cluster **2** is shown to have a lower reduction potential. The same discussion has been afforded in the bonding calculation of cluster **2**. Since cluster **2** is electron deficient, it is expected that the reduction is more feasible. From the feature of the LUMO, one can also conclude that the reduction mainly occurs at the Ru(5) centre. The HOMO, however, has noticeable a bonding interaction in the pentagonal bipyramidal moiety. The oxidation is expected to affect the stability of the pentagonal bipyramidal framework (see Figure 2). The cyclic voltammogram of cluster **4** in CH_2Cl_2 consists of irreversible reduction and oxidation processes at peaks located at $E_{pc} = -1.7$ and $E_{pa} = 0.76$ V, respectively. No evidence for the reversibility of either redox couple was observed when the scan rate was increased to 1 V s^{-1}. Controlled potential coulometry is run at 0.9 V, and indicates an overall consumption of two electrons per molecule. According to the similar relative peak currents of the cathodic and anodic electron transfer processes, we would assume that both reduction and oxidation steps involve two electrons per molecule. It is important to note that in the backscan after traversing the cathodic peak, new daughter peaks -0.82 and -0.13 V arise; these are clearly due to fast reorganization reactions of the instantaneously electrogenerated dianionic complex $\mathbf{4}^{2-}$. This process is akin to an ECEC or EEC reaction.

Conclusion

The deoxygenation chemistry of triruthenium methoxynitrido carbonyl cluster, $[Ru_3(CO)_9(\mu_3\text{-}CO)(\mu_3\text{-}NOMe)]$ has been studied in detail to give the coordinated nitrido or nitrene ligands. This work describes examples of the formation of a variety of cluster derivatives bearing alkyne ligands. The

0947-6539/01/0701-0268 $ 17.50+.50/0 *Chem. Eur. J.* **2001**, *7*, No. 1

isolation of $[Ru_3(CO)_9(\mu_3\text{-NOMe})(\mu_3\text{-}\eta^2\text{-PhC}_2\text{Ph})]$ (**1**) in high yields has afforded us an opportunity to study their reactivities in detail. Thermolysis of such a cluster with excess $[Cp^*Co(CO)_2]$ initiates the formation of a pentaruthenium μ_5-nitrido cluster **2**, in which the five metal atoms are arranged in a novel "spiked" square-planar framework. This cluster is rather rare, as it has four electrons less than expected; however, it is quite stable upon isolation. The alkyne ligand plays a special role in the assembly of this higher cluster of ruthenium. This is strongly suggested by the observation that the ligand can adopt the quadruply bridging bonding mode. The μ_5-nitrido N atom exhibits a signal in the ^{15}N NMR spectrum at an unusually low frequency; this is a counterexample to the "compression-deshielding" correlation.[47, 48] In addition, the reaction provides a striking example of the chemical activation of an μ_3-NOMe group upon coupling with CO and alkyne ligands to give metallapyrrolidone complexes in moderate yields. Another parallel process of C–H activation of the methyl group in the C_5Me_5 ligand is observed in cluster **4**. Crystal structure analysis revealed that the ligand bridges the Ru–Ru bond in **4** through both "alkene" carbons and the NOMe nitrogen atom. This mode of attachment gives each metal a formal 18-electron count and confers high thermal and chemical stability on the complex.

Experimental Section

General procedures: All reactions and manipulations were carried out under argon by using standard Schlenk techniques, except for the chromatographic separations. Solvents were purified by standard procedures and distilled prior to use. All chemicals, unless otherwise stated, were purchased commercially and used as received. $[Ru_3(CO)_9(\mu_3\text{-CO})(\mu_3\text{-NOMe})]$,[53] $[Ru_3(CO)_9(\mu_3\text{-NOMe})(\mu_3\text{-}\eta^2\text{-PhC}_2\text{Ph})]$[10] and $[PPN][^{15}NO_2]$[55] were prepared by the literature methods. Reactions were monitored by analytical thin-layer chromatography (Merck Kieselgel $60\,F_{254}$) and the products were separated by thin-layer chromatography on plates coated with silica (Merck Kieselgel $60\,GF_{254}$). Infrared spectra were recorded on a Bio-Rad FTS-7 IR spectrometer, with 0.5 mm calcium fluoride solution cells. ^1H NMR spectra were recorded on a Bruker DPX 300 NMR spectrometer with CD_2Cl_2 and referenced to $SiMe_4$ ($\delta = 0$), ^{15}N NMR spectra on a Bruker DPX 500 NMR spectrometer with $CDCl_3$ as the solvent and liquid NH_3 as a reference. The two-dimensional ^1H EXSY spectrum was obtained on a Bruker DPX 500 NMR spectrometer at 298 K by using the following parameters: spectrometer frequency 500 MHz, mixing time 100 ms, sweep width 4251.701 Hz with 1024 data points in the f_2 dimension and 256 data points in the f_1 dimension, acquisition time 0.120 s with 4 scans. Zero-filling in f_1 was applied to the final spectrum to yield a 1024×512 data set. Positive and negative ionization fast atom bombardment (FAB) mass spectra were recorded on a Finnigan MAT 95 mass spectrometer, with *m*-nitrobenzyl alcohol or α-thioglycerol as matrix solvents. Electronic absorption spectra were obtained on a Hewlett-Packard 8453 diode array UV/Vis spectrophotometer by using quartz cells with 1 cm path length at room temperature. Microanalyses were performed by Butterworth Laboratories (UK).

Reaction of $[Ru_3(CO)_9(\mu_3\text{-NOMe})(\mu_3\text{-}\eta^2\text{-PhC}_2\text{Ph})]$ (1) with $[Cp^*Co(CO)_2]$: A solution of **1** (200 mg, 0.257 mmol) in THF (60 mL) was heated with 2 equivalents of $[Cp^*Co(CO)_2]$ (129 mg, 0.514 mmol) under an argon atmosphere. The colour of the solution changed to dark brown upon heating under reflux for 12 hours. The solvent was removed in vacuo. The residue was redissolved in a small amount of CH_2Cl_2 and separated by preparative TLC plates by using *n*-hexane/dichloromethane (2:1, v/v) as the eluent. Four new products, as well as several known compounds, were isolated in the following order of elution: trace amounts of red $[Ru_4(CO)_{12}(\mu_4\text{-}\eta^2\text{-PhC}_2\text{Ph})]$[18] ($R_f = 0.85$), yellow $[Ru_4(CO)_9(\mu\text{-CO})_2(\mu_4\text{-NOMe})(\mu_4\text{-}\eta^2\text{-PhC}_2\text{Ph})]$[10] ($R_f = 0.83$), purple $[Ru_2Co(CO)_6(\mu_3\text{-CO})(\eta^5\text{-}C_5Me_5)(\mu_3\text{-NH})]$[16] ($R_f = 0.80$), brown $[Ru_5(CO)_8(\mu\text{-CO})_3(\eta^5\text{-}C_5Me_5)(\mu_5\text{-N})(\mu_4\text{-}\eta^2\text{-PhC}_2\text{Ph})]$ (**2**) ($R_f = 0.75$, 26.4 mg, 0.023 mmol, 15 %), yellow $[Ru_4(CO)_9(\mu\text{-CO})_2(\mu_4\text{-NH})(\mu_4\text{-}\eta^2\text{-PhC}_2\text{Ph})]$[19] ($R_f = 0.70$, 17.4 mg, 0.019 mmol, 10 %), brown $[Ru_3Co(CO)_6(\mu\text{-CO})_2(\eta^5\text{-}C_5Me_5)(\mu_4\text{-NH})(\mu_4\text{-}\eta^2\text{-PhC}_2\text{Ph})]$[16] ($R_f = 0.65$, 28.2 mg, 0.031 mmol, 12 %), green $[Ru_3Co_2(CO)_7(\mu_3\text{-CO})(\eta^5\text{-}C_5Me_5)_2(\mu_3\text{-NH})\{\mu_4\text{-}\eta^8\text{-}C_6H_4C(H)C(Ph)\}]$ (**3**) ($R_f = 0.48$, 8.54 mg, 0.0077 mmol, 3 %), orange $[Ru_3(CO)_7(\mu\text{-}\eta^6\text{-}C_5Me_4CH_2)\{\mu\text{-}\eta^3\text{-PhC}_2(Ph)C(O)N(OMe)\}]$ (**4**) ($R_f = 0.25$, 59.1 mg, 0.067 mmol, 26 %) and pale yellow $[Ru_2(CO)_6\{\mu\text{-}\eta^3\text{-PhC}_2(Ph)C(O)N(OMe)\}]$ (**5**) ($R_f = 0.20$, 19.2 mg, 0.031mmol, 8 %). Elemental analysis calcd (%) for $C_{35}H_{25}NO_{11}Ru_3$ **2**: C 36.84, H 2.19, N 1.23; found: C 36.9, H 2.3, N 1.2; elemental analysis calcd (%) for $C_{42}H_{41}NO_8Co_2Ru_3$ **3**: C 45.49, H 3.70, N 1.26; found: C 45.3, H 3.6, N 1.4; elemental analysis calcd (%) for for $C_{33}H_{27}NO_9Ru_3$ **4**: C 44.80, H 3.05 N 1.58; found: C 44.9, H 3.2, N 1.5.

Reaction of 1 with pentamethylcyclopentadiene and 1,3-cyclohexadiene: A solution of complex **1** (30 mg, 0.039 mmol) in THF (30 mL) was heated with 1 drop each of pentamethylcyclopentadiene and 1,3-cyclohexadiene under an argon atmosphere. The initial yellow solution changed to brown upon heating under reflux. After 12 hours, the reaction mixture was dried under reduced pressure. The residue was redissolved in CH_2Cl_2 (2 mL) and separated by preparative TLC, with *n*-hexane/CH_2Cl_2 (2:1, v/v) as the eluent to afford one brown band **2** ($R_f = 0.75$) in 4 % yield (1.06 mg, 0.0009 mmol). The reaction of complex **1** with only a drop of pentamethylcyclopentadiene in similar conditions was attempted. The reaction was monitored by IR and spot TLC; however, no change was observed. About 75 % of the starting material was recovered upon separation on preparative silica plates.

Reaction of 4 with $[Ru_3(CO)_{12}]$: Compound **4** (30 mg, 0.034 mmol) and a slight excess $[Ru_3(CO)_{12}]$ (26.0 mg, 0.041 mmol) were dissolved in *n*-octane (30 mL). The orange solution was heated to reflux for 4 hours. The solvent was then removed under reduced pressure and the residue was purified by chromatography on TLC plates with *n*-hexane/CH_2Cl_2 (6:1, v/v) as eluent. Two consecutive bands were eluted, $[Ru_3(CO)_{12}]$ ($R_f = 0.95$, 12.1 mg, 0.019 mmol) and $[Ru_6(\mu_3\text{-H})(CO)_{12}(\mu\text{-CO})(\mu_4\text{-}\eta^2\text{-CO})_2(\eta^5\text{-}C_5Me_5)]$[44] ($R_f =$ 0.60, 2.56 mg, 0.0022 mmol, 3 %).

Reaction of 1 with $[Cp^*Co(CO)I_2]$: Complex **1** (50 mg, 0.13 mmol) and $[Cp^*Co(CO)I_2]$ (36.7 mg, 0.077 mmol) were dissolved in THF (50 mL). The dark purple solution was heated at 65 °C for 2 hours, which resulted in the formation of a deep brown solution. The solvent was removed under reduced pressure and the residue separated by preparative TLC with *n*-hexane/CH_2Cl_2 (3:2, v/v) as the eluent. The only product isolated was $[Ru_3Co(CO)_5(\eta^5\text{-}C_5Me_5)(\mu_4\text{-N})(\mu_3\text{-}\eta^2\text{-PhC}_2\text{Ph})(\mu\text{-I})_2I]$ (**6**) ($R_f = 0.40$, 2.33 mg, 0.0019 mmol, 3 %) accompanied by decomposition. Elemental analysis calcd (%) for $C_{29}H_{25}NO_5I_3CoRu_3$ **6**: C 28.76, H 2.07, N 1.16; found: C 28.9, H 2.1, N 1.1.

Electrochemical studies: Electrochemical measurements were carried out by using an EG & G Princeton Applied Research (PAR) Model 273A potentiostat/galvanostat connected to an interfaced computer that employed PAR 270 electrochemical software. Cyclic voltammograms were obtained with a gas-sealed (argon) two-compartment cell, equipped with a glassy carbon working electrode (Bioanalytical), platinum wire auxiliary (Aldrich) and $Ag/AgNO_3$ reference (Bioanalytical) electrodes at room temperature. *n*-Tetrabutylammonium hexafluorophosphate (TBAHFP; 0.1 mol dm^{-3}) in anhydrous deoxygenated CH_2Cl_2 was used as a supporting electrolyte. Ferrocene was added at the end of each experiment as an internal standard.[56] Potential data (vs $Ag/AgNO_3$) were checked against the ferrocene $(0/+1)$ couple; under the actual experimental conditions the ferrocene/ferrocenium couple is located at $+0.18$ V in dichloromethane. Bulk electrolyses were carried out in a gas-tight cell consisting of three chambers separated at the bottom by fine frits, with a carbon cloth (80 mm^2) working electrode in the middle, and $Ag/AgNO_3$ reference and Pt gauze auxiliary electrodes in the lateral chambers. The working potential (E_w) for reduction and oxidation processes was about 0.15 V negative and positive of the corresponding electrode potential (E_p), respectively; all coulometric experiments were completed in duplicate.

Crystallography: Crystals suitable for X-ray analyses were glued on glass fibres with epoxy resin or sealed in 0.3 mm glass capillary. Intensity data were collected at ambient temperature either on a Rigaku-AFC7R diffractometer (complex **2**) or a MAR research image plate scanner

(complexes **3**, **4** and **6**) equipped with graphite-monochromated $Mo_{K\alpha}$ radiation ($\lambda = 0.710\ 73$ Å) by using $\omega - 2\theta$ and ω scan types, respectively. Details of the intensity data collection and crystal data are given in Table 8. The diffracted intensities were corrected for Lorentz and polarization effects. The Ψ scan method was employed for semi-empirical absorption corrections for **2**;[57] however, an approximation to absorption correction by inter-image scaling was applied for **3**, **4** and **6**. Scattering factors were taken from ref. [58a] and anormalous dispersion effects[58b] were included in F_c.

Table 8. Crystal data and data collection parameters for compounds **2** – **4** and **6**

	2	**3**·1.5 C_7H_8	**4**	**6**
formula	$C_{35}H_{25}NO_{11}Ru_5$	$C_{52.5}H_{53}NO_8Co_2Ru_3$	$C_{33}H_{27}NO_9Ru_3$	$C_{29}H_{25}NO_5I_3CoRu_3$
M_w	1140.93	1247.07	884.79	1210.38
colour, habit	brown, block	green, block	orange, plate	dark brown, block
crystal size [mm]	0.21 × 0.25 × 0.28	0.12 × 0.20 × 0.21	0.10 × 0.32 × 0.32	0.12 × 0.19 × 0.21
crystal system	monoclinic	triclinic	monoclinic	monoclinic
space group	$P2_1/c$ (no. 14)	$P\bar{1}$ (no. 2)	$P2_1/c$ (no. 14)	$P2_1/n$ (no. 14)
a [Å]	10.319(3)	12.750(1)	12.639(1)	10.348(1)
b [Å]	30.804(4)	12.970(1)	11.701(1)	18.348(2)
c [Å]	11.703(4)	18.838(2)	22.673(2)	17.582(3)
α [°]		91.17(2)		
β [°]	101.74(3)	101.52(2)	93.72(2)	91.83(2)
γ [°]		118.83(2)		
U [Å^3]	3642(1)	2649.3(8)	3346.0(5)	3336.5(6)
Z	4	2	4	4
ρ_{calcd} [g cm^{-3}]	2.080	1.563	1.756	2.409
μ ($Mo_{K\alpha}$) [cm^{-1}]	20.87	15.00	13.91	46.36
reflections collected	5194	20751	28161	28792
unique reflections	4883	8794	5359	4490
observed reflections [$I > 1.5\sigma(I)$]	4313	6841	3015	2795
R	0.029	0.045	0.054	0.048
R'	0.032	0.050	0.048	0.045
Goodness of fit, S	1.91	1.48	1.24	1.30

The structures were solved by direct methods (SIR92[59] for **2**, **3** and SHELX86[60] for **4**, **6**) and expanded by Fourier-difference techniques. Atomic coordinates and thermal parameters were refined by full-matrix least-squares analysis on F, with the ruthenium atoms and non-hydrogen atoms being refined anisotropically. The hydrogen atom of the nitrene moieties and metal hydride were located by Fourier difference synthesis, while those of the organic moieties were generated in their ideal positions (C–H 0.95 Å). Calculations were performed on a Silicon-Graphics computer, using the program package TEXSAN.[61] Crystallographic data (excluding structure factors) for the structures reported in this paper have been deposited with the Cambridge Crystallographic Data Centre as supplementary publication no. CCDC-142397 to CCDC-142400. Copies of the data can be obtained free of charge on application to CCDC, 12 Union Road, Cambridge CB2 1EZ, UK (fax: (+44) 1223-336-033; e-mail: deposit @ccdc.cam.ac.uk).

Acknowledgements

We gratefully acknowledge financial support from the Hong Kong Research Grants Council and the University of Hong Kong. E.N.-M.H. acknowledges the receipt of a postgraduate studentship, Swire Scholarship 1998 – 2000, Hung Hing Ying Scholarship 1998 – 2000 and Epson Foundation Scholarship 2000 – 2001 administered by the University of Hong Kong and Michael Gale Scholarship 1998 – 99 awarded by the University of Hong Kong and Hong Kong Telecom Foundation. We wish to thank Dr. G. D. Brown for his helpful discussion on the two-dimensional EXSY spectral data.

[1] P. Braunstein, J. Rosé in *Catalysis by Di- and Polynuclear Metal Cluster Complexes: Heterometallic Clusters for Heterogeneous Catalysis* (Eds.: R. D. Adams, F. A. Cotton), Wiley-VCH, New York, **1998**, pp. 443 – 508.
[2] P. Braunstein, J. Rosé in *Comprehensive Organometallic Chemistry II*, *Vol. 10* (Eds.: E. W. Abel, F. G. A. Stone, G. Wilkinson), Pergamon Press, Oxford, **1995**, pp. 351 – 385.
[3] P. Braunstein, J. Rosé in *Metal Clusters in Chemistry* (Eds: P. Braunstein, P. R. Raithby, L. A. Oro), Wiley-VCH, Weinheim, Germany, **1999**, *2*, pp. 616 – 677.
[4] E. Rosenberg, R. M. Laine in *Catalysis by Di- and Polynuclear Metal Complexes* (Eds.: R D. Adams, F. A. Cotton), Wiley-VCH, New York, **1998**, pp. 1 – 38.
[5] G. Süss-Fink, M. Jahncke in *Catalysis by Di- and Polynuclear Metal Complexes* (Eds.:, R. D. Adams, F. A. Cotton), Wiley-VCH, New York, **1998**, pp. 167 – 248.
[6] F. G. A. Stone, *Angew. Chem.* **1984**, *96*, 147; *Angew. Chem. Int. Ed. Engl.* **1984**, *23*, 89 – 172.
[7] H. Vahrenkamp, *Adv. Organomet. Chem.* **1983**, *22*, 169 – 208.
[8] J.-S. Song, S.-H. Han, S. T. Nguyen, G. L. Geoffroy, A. L. Rheingold, *Organometallics* **1990**, *9*, 2386 – 2395.
[9] E. N.-M. Ho, W.-T. Wong, *J. Chem. Soc. Dalton Trans.* **1998**, 513 – 514.
[10] E. N.-M. Ho, W.-T. Wong, *J. Chem. Soc. Dalton Trans.* **1998**, 4215 – 4228.
[11] S.-H. Han, G. L. Geoffroy, A. L. Rheingold, *Organometallics* **1986**, *5*, 2561 – 2563.
[12] S.-H. Han, G. L. Geoffroy, A. L. Rheingold, *Organometallics* **1987**, *6*, 2380 – 2386.
[13] K. K.-H. Lee, W.-T. Wong, *J. Chem. Soc. Dalton Trans.* **1996**, 1707 – 1720.
[14] K. K.-H. Lee, W.-T. Wong, *J. Organomet. Chem.* **1995**, *503*, C43 – C45.
[15] K. K.-H. Lee, W.-T. Wong, *Inorg. Chem.* **1996**, *35*, 5393 – 5395.
[16] E. N.-M. Ho, W.-T. Wong, *Eur. J. Inorg. Chem.*, in press.
[17] E. N.-M. Ho, W.-T. Wong, unpublished results.
[18] B. F. G. Johnson, J. Lewis, B. E. Reichert, K. T. Schorpp, G. M. Sheldrick, *J. Chem. Soc. Dalton Trans.* **1977**, 1417 – 1419.
[19] M. L. Blohm, W. L. Gladfelter, *Organometallics* **1986**, *5*, 1049 – 1051.
[20] W. L. Gladfelter, *Adv. Organomet. Chem.* **1985**, *24*, 41 – 86.
[21] S. Martinengo, G. Ciani, A. Sironi, B. T. Heaton, J. Mason, *J. Am. Chem. Soc.* **1979**, *101*, 7095 – 7097.
[22] S. Martinengo, G. Ciani, A. Sironi, *J. Am. Chem. Soc.* **1982**, *104*, 328 – 330.
[23] M. R. Churchill, F. J. Hollander, J. P. Hutchinson, *Inorg. Chem*. **1977**, *16*, 2655 – 2659.
[24] M. D. Curtis, K. R. Han, W. M. Butler, *Inorg. Chem.* **1980**, *19*, 2096 – 2101.
[25] D. M. P. Mingos, D. J. Wales, *Introduction to Cluster Chemistry*, Prentice-Hall, New Jersey, **1990**.
[26] D. G. Evans, D. M. P. Mingos, *Organometallics* **1983**, *2*, 435 – 447.
[27] Density functional calculations at the B3LYP level were performed on the model cluster $[Ru_5(CO)_8(\mu\text{-}CO)_3(\eta^5\text{-}C_5H_5)(\mu_5\text{-}N)(\mu_4\text{-}\eta^2\text{-}HC_2H)]$ on the basis of the experimentally determined geometry. The basis set used for C, N, O and H atoms was 6 – 31 G, while an effective core potential with a LanL2DZ basis set was employed for Ru and Co.
[28] A. Reed, L. A. Curtiss, F. Weinhold, *Chem. Rev.* **1988**, *88*, 899 – 926.
[29] K. B. Wiberg, *Tetrahedron* **1968**, *24*, 1083 – 1096.
[30] G. Schaftenaar, *Molden v.35*, CAOS/CAMM Centre Nijmegen, Toernooiveld, Nijmegen (Netherlands) **1999**.
[31] P. C. Steinhardt, W. L. Gladfelter, A. D. Harley, J. R. Fox, G. L. Geoffroy, *Inorg. Chem.* **1980**, *19*, 332 – 339.
[32] P. A. Corrigan, R. S. Dickson, G. D. Fallon, L. J. Michel, C. Mok, *Aust. J. Chem.* **1978**, *31*, 1937 – 1951.

  0947-6539/01/0701-0270 $ 17.50+.50/0

[33] S. Sergio, F. Carlo, C.-V. Angiola, G. Carlo, *Angew. Chem.* **1987**, *99*, 84–86; *Angew. Chem. Int. Ed. Engl.* **1987**, *26*, 68–70.
[34] K. J. Kerry, J. J. Barker, S. A. R. Knox, A. G. Orpen, *J. Chem. Soc. Dalton Trans.* **1996**, 975–988.
[35] H. G. Ang, S. G. Ang, S. Du, *J. Chem. Soc. Dalton Trans.* **1999**, 2963–2970.
[36] M. I. Bruce, J. R. Hinchliffe, P. A. Humphrey, R. J. Surynt, B. W. Skelton, A. H. White, *J. Organomet. Chem.* **1998**, *552*, 109–125.
[37] I. J. Hart, J. C. Jeffery, M. J. Grosse-Ophoff, F. G. A. Stone, *J. Chem. Soc. Dalton Trans.* **1988**, 1867–1877.
[38] A. Habiyakare, E. A. C. Lucken, G. Bernardinelli, *J. Chem. Soc. Dalton Trans.* **1992**, 2591–2599.
[39] S. P. Tunik, E. V. Grachova, V. R. Denisov, G. L. Starova, A. B. Nikol'skii, F. M. Dolgushin, A. I. Yanovsky, Y. T. Struchkov, *J. Organomet. Chem.* **1997**, *536–537*, 339–343.
[40] R. D. Adams, G. Chen, J. Yin, *Organometallics* **1991**, *10*, 1278–1282.
[41] V. S. Kaganovich, M. I. Rybinskaya, Z. A. Kerzina, F. M. Dolgushin, A. I. Yanovsky, Y. T. Struchkov, P. V. Petrovskii, E. Kolehmainen, J. Kivikoski, J. Valkonen, K. Laihia, *J. Organomet. Chem.* **1996**, *518*, 115–119.
[42] A. J. Blake, P. J. Dyson, B. F. G. Johnson, S. Parsons, D. Reed, D. S. Shephard, *Organometallics* **1995**, *14*, 4199–4208.
[43] F. Bottomley, G. O. Egharevba, I. J. B. Lin, P. S. White, *Organometallics* **1985**, *4*, 550–553.
[44] E. Kolehmainen, K. Rissanen, K. Laihia, Z. A. Kerzina, M. I. Rybinskaya, M. Nieger, *J. Organomet. Chem.* **1996**, *524*, 219–223.
[45] J. F. Halet, J. Y. Saillard, R. Lissillour, M. McGlinchey, G. Jaouen, *Inorg, Chem.* **1985**, *24*, 218–224.
[46] D. M. P. Mingos, *Acc. Chem. Res.* **1984**, *17*, 311–319.
[47] M. L. Blohm, W. L. Gladfelter, *Organometallics* **1985**, *4*, 45–52.
[48] D. E. Fjare, W. L. Gladfelter, *J. Am. Chem. Soc.* **1984**, *106*, 4799–4810.
[49] J. Mason, *J. Am. Chem. Soc.* **1991**, *113*, 24–26.
[50] J. Mason, *J. Am. Chem. Soc.* **1991**, *113*, 6056–6062.
[51] T. Jaeger, S. Aime, H. Vahrenkamp, *Organometallics* 1986, **5**, 245–252.
[52] A. J. Gordon, R. A. Ford, *The Chemist Companion: A Handbook of Practical Data, Techniques, and References*, Wiley, New York, **1973**, p. 299.
[53] R. E. Stevens, W. L. Gladfelter, *J. Am. Chem. Soc.* **1982**, *104*, 6454–6457.
[54] S. R. Drake, *Polyhedron* **1990**, *9*, 455–474.
[55] R. E. Stevens, W. L. Gladfelter, *Inorg. Chem.* **1983**, *22*, 2034–2042.
[56] G. Gritzner, J. Kute, *Pure Appl. Chem.* **1984**, *56*, 461–466.
[57] A. C. T. North, D. C. Phillips, F. S. Mathews, *Acta Crystallogr. Sect. A* **1968**, *24*, 351–359.
[58] a) D. T. Cromer, J. T. Waber, *International Tables for X-ray Crystallography Vol. 4*, Kynoch, Birmingham, **1974**, Table 2.2B; b) D. T. Cromer, J. T. Waber, *International Tables for X-ray Crystallography Vol. 4*, Kynoch, Birmingham, **1974**, Table 2.3.1.
[59] A. Altomare, M. C. Burla, M. Camalli, M.Cascarano, C. Giacovazzo, A. Guagliardi, G. Polidori, *J. Appl. Crystallogr.* **1992**, *25*, 310–318.
[60] G. M. Sheldrick, *Crystallographic Computing 3* (Eds.: G. M. Sheldrick, C. Kruger, R. Goddard), Oxford University Press, **1985**, p. 175.
[61] TEXSAN, Crystal Structure Analysis Package, Molecular Structure Corporation, Houston, TX, **1985** and **1992**.

Received: April 05, 2000 [F2405]